

CCD time-series photometry of the globular cluster NGC 5053: RR Lyrae, Blue Stragglers and SX Phoenicis stars revisited*

A. Arellano Ferro¹, Sunetra Giridhar², D.M. Bramich³

¹*Instituto de Astronomía, Universidad Nacional Autónoma de México, México: armando@astroscu.unam.mx*

²*Indian Institute of Astrophysics, Koramangala 560034, Bangalore, India: giridhar@iiap.res.in*

³*European Southern Observatory, Karl-Schwarzschild-Straße 2, 85748 Garching bei München, Germany: dan.bramich@hotmail.co.uk*

Accepted . Received ; in original form

ABSTRACT

We report the results of CCD V , r and I time-series photometry of the globular cluster NGC 5053. New times of maximum light are given for the eight known RR Lyrae stars in the field of our images and their periods are revised. Their V light curves were Fourier decomposed to estimate their physical parameters. A discussion on the accuracy of the Fourier-based iron abundances, temperatures, masses and radii is given. New periods are found for the 5 known SX Phe stars and a critical discussion of their secular period changes is offered. The mean iron abundance for the RR Lyrae stars is found to be $[\text{Fe}/\text{H}] \sim -1.97 \pm 0.16$ and lower values are not supported by the present analysis. The absolute magnitude calibrations of the RR Lyrae stars yield an average true distance modulus of 16.12 ± 0.04 or a distance of 16.7 ± 0.3 kpc. Comparison of the observational CMD with theoretical isochrones indicates an age of 12.5 ± 2.0 Gyrs for the cluster. A careful identification of all reported Blue Stragglers (BS) and their V, I magnitudes leads to the conclusion that BS12, BS22, BS23 and BS24 are not BS. On the other hand, three new BS are reported. Variability was found in seven BS, very likely of the SX Phe type in five of them, and in one red giant star. The new SX Phe stars follow established PL relationships and indicate a distance in agreement with the distance from the RR Lyrae stars.

Key words: Globular Clusters: NGC 5053 – Variable Stars: RR Lyrae, Blue Stragglers, SX Phoenicis.

1 INTRODUCTION

Recent numerical methods in the analysis of stellar CCD images have proven to be very powerful in isolating faint stars and performing accurate photometry even in very crowded fields, such as in the central regions of globular clusters (Bramich 2008, Bramich et al. 2005; Alard 2000; Alard & Lupton 1998). In a series of papers we have taken advantage of these mathematical techniques to study the known variable stars and to search for new ones in several globular clusters of assorted metallicities (Arellano Ferro et al. 2008a; 2008b; 2004, Lázaro et al. 2006). In particular we used the Fourier decomposition technique to estimate fundamental physical parameters of the RR Lyrae stars and

we searched for eclipsing binaries and variability among the blue stragglers. The calculation of the iron content $[\text{Fe}/\text{H}]$ and absolute magnitude M_V lead to a linear M_V - $[\text{Fe}/\text{H}]$ relationship (Arellano Ferro et al. 2008b) that is in agreement with independent estimations from different empirical techniques (e.g. Cacciari & Clementini 2003; Chaboyer 1999).

The globular cluster NGC 5053 (R.A.(J2000)= $13^{\text{h}}16^{\text{m}}27^{\text{s}}.3$, DEC(J2000)= $+17^{\circ}41'52''$, $l = 335.7$, $b = +78.9$) is located in the intermediate Galactic halo ($Z = 16.1$ kpc, $R_G=16.9$ kpc) and it is one of the most metal deficient clusters; $[\text{Fe}/\text{H}] = -2.1$ (Rutledge et al. 1997). It is a rather disperse and well resolved system which allows high quality photometry even in the central regions. Such characteristics place this stellar system close to the grey region between globular clusters and open clusters. Nevertheless it was classified as a globular cluster mainly due to its high galactic latitude and the presence of faint stars and some

* Based on observations collected at the Indian Astrophysical Observatory, Hanle, India.

variables (Cuffey 1943, Baade 1928). The cluster has been the subject of detailed photometric studies and the most recent ones, already in the CCD era, conducted detailed studies of known RR Lyrae stars (Nemec, Mateo & Schombert 1995) and the identification of 28 blue stragglers (Nemec & Cohen 1989; Sarajedini & Milone 1995) among which 5 are known to be SX Phe variables (Nemec et al. 1995).

In the present paper we perform standard V , I and instrumental r CCD photometry for nearly 6500 stars in the field of NGC 5053 and perform the Fourier light curve decomposition of the known RR Lyrae stars. We also search for variability among Blue Straggler (BS) stars and revisit the known SX Phe stars previously studied by Nemec et al. (1995), in an attempt to refine their periodicities in order to discuss their period changes and to use them as independent indicators of the distance to the cluster. Finally we report five new SX Phe stars, three new BS stars, and one new red giant variable (RGV).

The paper is organised as follows: in § 2 we describe the observations, data reductions and transformations to the standard photometric system. In § 3 a period analysis of the RR Lyrae stars is performed. In § 4 the V light curves of the RR Lyrae stars are Fourier decomposed and their physical parameters are estimated. In § 5 the periods and secular period changes of the SX Phe stars are discussed as well as the BS nature of previously reported BS stars. In § 6 a search for new variables is carried out and the new variables are described. In § 7 the distance and age of NGC 5053 are discussed and in § 8 we summarise our conclusions.

2 OBSERVATIONS AND REDUCTIONS

The observations employed in the present work were performed using the Johnson V , R and I filters and obtained with the 2.0m telescope of the Indian Astronomical Observatory (IAO), Hanle, India, located at 4500m above sea level, during several runs between April 2006 and January 2009. The cluster was observed during a total of 10 nights and 151 images were gathered in the Johnson V , 139 in R and 13 in I . The average seeing was ~ 1 arcsec. The detector was a Thompson CCD of 2048×2048 pixels with a pixel scale of 0.17 arcsec/pix and a field of view of approximately $11. \times 11$. arcmin.

Difference image analysis (DIA) is a powerful technique allowing accurate PSF photometry of CCD images, even in very crowded fields (Alard & Lupton 1998; Alard 2000; Bramich et al. 2005). In the present study, we used a pre-release version of the DANDIA¹ software for the DIA (Bramich et al., in preparation), which employs a new algorithm for determining the convolution kernel matching a pair of images of the same field (Bramich 2008). This algorithm was applied to a set of V , R and I images of NGC 5053 in order to obtain accurate time-series photometry and to search for new variable stars down to $V \sim 19.5$ mag.

For a brief description of the DIA procedure the reader is referred to § 2 of the paper by Arellano Ferro et al. (2008b)

The instrumental v and i magnitudes were converted to the Johnson V and I standard system

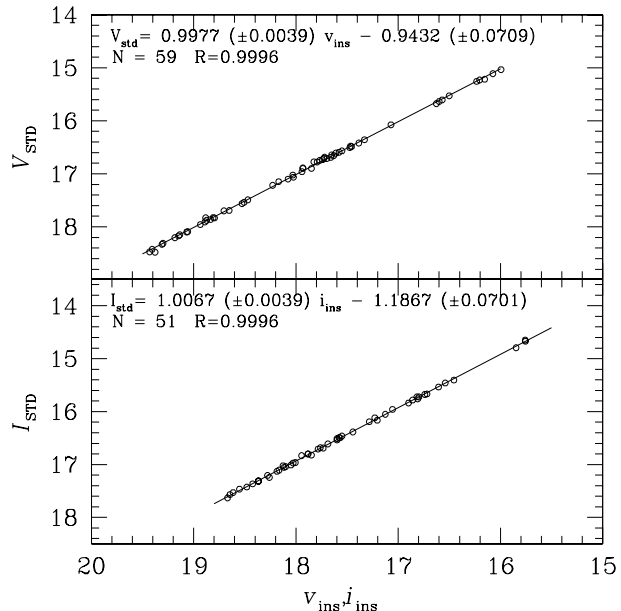


Figure 1. Photometry transformation relations calculated using the standard stars in V and I from the collection of Stetson (2000).

Table 1. Periods of the known RR Lyrae stars in NGC 5053. Most periods have been revised in this work (column 2) and new times of maximum light were calculated (column 3). The predicted periods using the periods and period change rates of Nemec (2004) are listed in column 4.

ID	Period (days)	Times of Maximum (+240 0000)	Predicted Period (days)
V2	0.378960	53832.325 53862.270	0.378956
V3	0.592950	53862.158	0.592946
V4	0.667073 ¹	54202.326	0.667079
V5	0.714860 ¹	53833.300	0.714866
V6	0.292185	53832.390 53833.265 53861.323 54201.400	0.292178
V7	0.351900	53828.721	0.351927
V8	0.362864	53833.259	0.362857
V10	0.77585 ¹	53833.259	0.775850

1. Nemec (2004)

using the collection of standards of Stetson (2000) (<http://www3.cadc-ccda.hia-ihp.nrc-cnrc.gc.ca/community/STETSON/standards>). For NGC 5053 we identified 59 V and 51 I standard stars in the field of the cluster and the transformations are shown in Fig. 1. The transformations were found to be linear and no colour term was found to be significant. The linear correlation coefficients were of the order of 0.999. The instrumental r magnitudes were retained in the instrumental system since no R standards were found in the literature.

¹ DANDIA is built from the DanIDL library of IDL routines available at <http://www.danidl.co.uk>

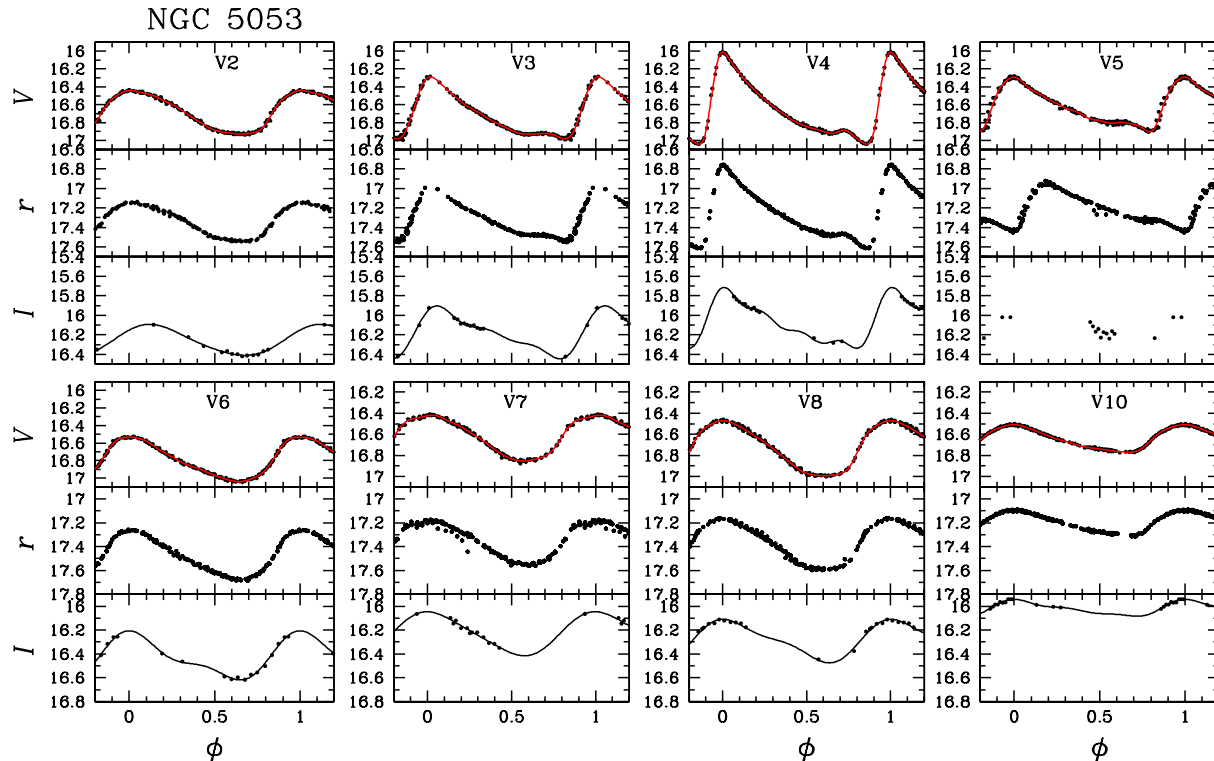


Figure 2. V, r, I light curves of the RR Lyrae stars in NGC 5053 phased with the new ephemerides from column 2 in Table 1.

Table 2. V, r, I magnitudes of the RR Lyrae, variable BS and new variable stars in NGC 5053 (extract).

Star	HJD _V	V	HJD _r	r	HJD _I	I
V2	2453832.2276	16.898	2453832.2374	17.487	2454839.4620	16.399
V2	2453832.2334	16.876	2453832.2411	17.484	2454839.4500	16.395
V2	2453832.2484	16.800	2453832.2438	17.468	2454839.4272	16.380
V2	2453832.2525	16.772	2453832.2562	17.390	2454839.4389	16.365
V2	2453832.2626	16.689	2453832.2589	17.374	2454839.4724	16.419
...

3 THE RR LYRAE STARS

3.1 New ephemerides and times of maximum light of the RR Lyrae stars

Ten RR Lyrae stars are known in NGC 5053 (Clement et al. 2001) but only eight are in the field of our collection of images. Our light curves were originally phased with the ephemerides of Nemeč (2004). However, except for V5 and V10, we noticed that this produced poor quality folded light curves. To calculate the periods at the epoch of our observations we applied the phase dispersion minimisation technique (PDM) (Burke et al. 1970; Dwořetsky 1983). The periods that we found are listed in column 2 of Table 1. In most cases the new periods differ substantially from those from Nemeč (2004) (e.g. V3, V7 and V8) while for V5 and V10 the periods coincide within 3×10^{-6} days; in these cases the periods from Mannino (1963) and Nemeč (2004) were adopted respectively. We have also estimated a number of epochs of maximum V light and these are listed in column 3 of Table 1.

In Fig. 2 the light curves in standard VI and instrumental r magnitudes are displayed. The vertical scale is the same for all stars and filters so that amplitude and brightness differences can be seen at a glance.

All our V, r and I photometry for the RR Lyrae stars is available in Table 2. Only a small portion of this table is shown in the printed version but a full version is available in electronic form.

3.2 Updated periods and period change rates for the RR Lyrae stars

A thorough analysis of the secular variations in the periods of the RR Lyrae stars in NGC 5053 was carried out by Nemeč (2004). Since only a few years have elapsed between the most recent data of Nemeč in 2002 and the earliest data from this paper in 2006, there is very little that we could add to Nemeč's O-C diagrams and/or the derived period change rates. We adopted his period change rates (column 11 of his Table 7) in order to predict the period at the average epoch

of our data. The predicted periods are listed in column 4 of Table 1. These predicted periods do not phase our light curves correctly in all cases, and in some cases there are substantial differences with the best periods found in this work (column 2), which were used to phase the light curves shown in Fig. 2. Therefore, it seems likely that the secular period changes quoted by Nemeč (2004) are overwhelmed by observational inaccuracies.

4 FOURIER DECOMPOSITION APPROACH TO THE PHYSICAL PARAMETERS OF RR LYRAE STARS

The red continuous curve in each of the V light curve panels of Fig. 2 is the Fourier fit to the data and it is mathematically represented by an equation of the form:

$$m(t) = A_o + \sum_{k=1}^N A_k \cos\left(\frac{2\pi}{P} k (t - E) + \phi_k\right), \quad (1)$$

where $m(t)$ are magnitudes at time t , P the period and E the epoch. A linear minimisation routine is used to fit the data with the Fourier series model, deriving the best fit values of the amplitudes A_k and phases ϕ_k of the sinusoidal harmonics. From the amplitudes and phases of the harmonics in eq. 1, the Fourier parameters are defined as: $\phi_{ij} = j\phi_i - i\phi_j$, and $R_{ij} = A_i/A_j$. The number of harmonics required for the proper fit of a given light curve depends on the quality of the data; basically on the scatter and the coverage of the light curve. We have fitted as many harmonics as possible as long as their amplitudes are significant. The magnitude-weighted mean magnitudes A_0 (or $\langle V \rangle$), the amplitudes and phases of the first four harmonics, which are relevant to the physical parameter calibrations described below, and the total number of harmonics employed (NH) are listed in Table 3.

In order to estimate the magnitude-weighted mean (I), the I -curves were also analysed using the Fourier decomposition by eq. 1 despite possessing a sparse phase coverage. The order of harmonics in this case was kept as low as possible until a smooth curve of similar appearance to the V light curve was obtained.

The Fourier fit parameters in V have been used to derive physical parameters of the RR Lyrae stars. To calculate $[\text{Fe}/\text{H}]$, and M_V for each individual star we followed the procedure described in the paper by Arellano Ferro et al. (2008b) where a detailed discussion on the Fourier approach, its limitations and advantages is given. We do not repeat that discussion here and instead the interested reader is referred to that paper. In the following subsections we briefly describe the transformations employed to calculate the iron content and the luminosity for both RRC and RRab stars. Fourier based calculations of the effective temperatures, radii and masses are also addressed.

4.1 The iron abundance $[\text{Fe}/\text{H}]$

NGC 5053 has often been considered as the most metal deficient globular cluster in the Galactic Halo. Zinn (1985) lists the cluster with $[\text{Fe}/\text{H}] = -2.58 \pm 0.27$ which corresponds to the value -2.4 ± 0.3 in the Cohen scale determined by Bell & Gustafsson (1983) via the comparison of synthetic

spectra with the observed spectra of stars in the cluster. Despite the large uncertainty, this value for $[\text{Fe}/\text{H}]$ is commonly found in the literature for NGC 5053. Considerable effort has been invested in the calculation of the metallicity of the cluster after those first estimates, and numerous values are found in the literature: Suntzeff, Kraft & Kinman (1988), from spectral analysis of the Ca H&K found -2.18 ± 0.06 and from the Mg 5130-5200Å band: -2.44 ± 0.21 ; Armandroff et al. (1992), from the analysis of the Ca II triplet in the 8500-8660Å region found -2.41 ± 0.12 . A detailed discussion on the iron abundance of NGC 5053 has been given by Geisler et al. (1995) from which it can be highlighted that the more recent determinations find considerably higher values of $[\text{Fe}/\text{H}]$. Geisler et al. (1995), from an analysis of medium resolution spectra of the Ca II triplet, found $[\text{Fe}/\text{H}] = -2.10 \pm 0.06$, and by reconsidering BVI data from Sarajedini & Milone (1995) and the Ca II triplet equivalent widths of Armandroff et al. (1992), find the values of -2.21 and -2.22 respectively. Finally, Geisler et al. conclude that a likely value of $[\text{Fe}/\text{H}]$ in NGC 5053 is -2.15 . Geisler et al. (1995) also argue that the lower metallicity limit for globular clusters in the Galaxy is -2.25 ± 0.10 . A more recent analysis of the Ca II triplet by Rutledge et al. (1997) derives a value of $\sim -2.10 \pm 0.07$ for the iron content of this cluster.

For the RRab stars, the calibration of Jurcsik & Kovács (1996) was employed:

$$[\text{Fe}/\text{H}]_J = -5.038 - 5.394 P + 1.345 \phi_{31}^{(s)}, \quad (2)$$

where $\phi_{31}^{(s)}$ is the phase in a sine series. The phase in a sine series $\phi_{31}^{(s)}$ is related to the phase in a cosine series $\phi_{31}^{(c)}$ via: $\phi_{jk}^{(s)} = \phi_{jk}^{(c)} - (j - k)\frac{\pi}{2}$. The standard deviation of this calibration is 0.14 dex (Jurcsik 1998).

The metallicity scale of the above equation was transformed into the ZW scale using the relation $[\text{Fe}/\text{H}]_J = 1.431[\text{Fe}/\text{H}]_{ZW} + 0.88$ (Jurcsik 1995).

Eq. 2 is applicable to RRab stars with a deviation parameter D_m , defined by Jurcsik & Kovács (1996) and Kovács & Kanbur (1998), not exceeding a proper limit. These authors suggest $D_m \leq 3.0$. D_m values for individual RRab stars are given in column 2 of Table 4. All stars fulfill the condition except V10 which is not included in the $[\text{Fe}/\text{H}]$ average. The iron abundances $[\text{Fe}/\text{H}]_{ZW}$ for the RRab stars are reported in Table 4

Mean values $[\text{Fe}/\text{H}]_{ZW} = -1.97 \pm 0.18$ for the RRC stars and $[\text{Fe}/\text{H}]_{ZW} = -1.76 \pm 0.13$ for the RRab stars were obtained. The problem of the Jurcsik & Kovács (1996) calibration of eq. 2 giving values of $[\text{Fe}/\text{H}]$ too large by ~ 0.2 - 0.3 dex for very metal poor stars has been discussed particularly for the RRab stars in NGC 5053 by Nemeč (2004), whose result $[\text{Fe}/\text{H}] = -1.73$ is very similar to ours (-1.76). This issue has also been pointed out by Jurcsik & Kovács (1996) themselves, Kovács (2002) and for other clusters by Cacciari et al. (2005) (M3), Lázaro et al. (2006) (M2), Arellano Ferro et al. (2008a) (NGC 5466) and Arellano Ferro et al. (2008b) (NGC 6366). It is also interesting to note that a good agreement between the Fourier and spectroscopic $[\text{Fe}/\text{H}]$ values for the LMC RR Lyrae stars was found by Gratton et al. (2004) and Di Fabrizio et al. (2005) after a systematic correction of ~ -0.2 dex was applied to the Fourier values.

Table 3. Fourier fit parameters for the V light curves.

RRc stars											
ID	HJD 2400000.0+	P (days)	A_0 σ_{A_0}	A_1 σ_{A_1}	A_2 σ_{A_2}	A_3 σ_{A_3}	A_4 σ_{A_4}	ϕ_{21} $\sigma_{\phi_{21}}$	ϕ_{31} $\sigma_{\phi_{31}}$	ϕ_{41} $\sigma_{\phi_{41}}$	NH
V2	53832.325	0.378955	16.697 0.001	0.246 0.001	0.045 0.001	0.025 0.001	0.010 0.001	4.596 0.030	2.827 0.052	1.660 0.126	8
V6	53832.390	0.292185	16.805 0.001	0.238 0.001	0.066 0.001	0.014 0.001	0.009 0.001	4.295 0.019	2.408 0.078	0.524 0.124	6
V7	53828.721	0.351900	16.635 0.001	0.220 0.001	0.031 0.001	0.012 0.001	0.010 0.001	4.895 0.040	2.956 0.103	1.873 0.124	6
V8	53833.259	0.362864	16.747 0.001	0.265 0.001	0.048 0.001	0.022 0.001	0.013 0.001	4.595 0.031	2.700 0.066	1.699 0.113	7
RRab stars											
V3	53826.573	0.592944	16.721 0.001	0.280 0.002	0.112 0.002	0.074 0.002	0.036 0.002	3.962 0.023	1.877 0.035	0.049 0.061	6
V4	53822.093	0.667075	16.658 0.005	0.352 0.001	0.174 0.001	0.122 0.001	0.084 0.001	3.943 0.009	1.905 0.013	6.247 0.018	10
V5	53829.726	0.7148605 ¹	16.639 0.002	0.230 0.002	0.100 0.002	0.065 0.002	0.032 0.003	4.078 0.033	2.153 0.051	0.514 0.086	8
V10	53833.259	0.77585 ²	16.653 0.001	0.121 0.001	0.034 0.001	0.009 0.001	0.005 0.001	4.190 0.023	2.697 0.073	2.091 0.134	6

1. Mannino (1963), 2. Nemeč (2004)

Table 4. Physical parameters for the RRab stars.

Star	D_m	$[\text{Fe}/\text{H}]_J$	$[\text{Fe}/\text{H}]_{ZW}$	$M_V(K)$	$\log(L/L_\odot)$	μ_0	D (kpc)
V3	1.5	-1.49	-1.65	0.57	1.711	16.091	16.53
V4	1.5	-1.85	-1.90	0.43	1.727	16.168	17.12
V5	0.8	-1.72	-1.82	0.47	1.712	16.111	16.68
V10	11.7	-1.31 ¹	-1.53 ¹	0.48	1.706	16.111	16.68
average		-1.64	-1.76 ²	0.49	1.714	16.120	16.75
σ		± 0.18	± 0.13	± 0.06	± 0.009	± 0.033	± 0.26

 1: value not included in the averages. 2: this value is to be decreased by ~ 0.2 - 0.3 dex to bring the Fourier results in agreement with spectroscopic values. See text for discussion.

Therefore, applying such correction to the mean value of $[\text{Fe}/\text{H}]$ for the RRab one obtains $[\text{Fe}/\text{H}]_{ZW} = -1.96 \pm 0.13$.

For the RRc stars, we used the calibration of Morgan et al. (2007);

$$[\text{Fe}/\text{H}]_{ZW} = 52.466 P^2 - 30.075 P + 0.131 \phi_{31}^{(c)2} - 0.982 \phi_{31}^{(c)} - 4.198 \phi_{31}^{(c)} P + 2.424, \quad (3)$$

where $\phi_{31}^{(c)}$ is the phase in a series of cosines, and P the period in days. This calibration provides iron abundances in the metallicity scale of Zinn & West (1984) (ZW) with a standard deviation of 0.14 dex. The iron abundances $[\text{Fe}/\text{H}]_{ZW}$ for the RRc stars are reported in Table 5. We find a value of $[\text{Fe}/\text{H}]_{ZW} = -1.97 \pm 0.18$ in excellent agreement with the value derived from the analysis of the RRab stars after the correction discussed above. The calibration of Morgan et al. (2007) has been applied to RRc stars in M15 (-2.12) (Arelano Ferro et al. 2006) and NGC 5466 (-1.92) (Arelano Ferro et al. 2008a) and has proven to yield values in very good agreement with generally accepted and well established values from different techniques.

In conclusion, the present results also support the fact that iron values obtained from the calibration of eq. 2 for RRab stars need to be corrected by about -0.2 to -0.3 dex. Guided by the result for RRc stars, we corrected the iron value for the RRab stars by -0.2 . The present result also indicates that while the cluster is certainly very metal-poor, the extreme deficiency ascribed to it earlier is not supported.

4.2 Visual absolute magnitudes and luminosities

The luminosity, or absolute magnitude, for the RRc stars was calculated using the empirical calibration of Kovács (1998)

$$M_V(K) = 1.261 - 0.961 P - 0.044 \phi_{21}^{(s)} - 4.447 A_4, \quad (4)$$

with a standard deviation of 0.042 mag.

To bring the scale of eq. 4 into agreement with the mean magnitude for the RR Lyrae stars in the LMC, $V_0 = 19.064 \pm 0.064$ (Clementini et al. 2003), it has been necessary to decrease the zero point by 0.2 ± 0.02 mag (Cacciari et al. 2005). The reported M_V values in Table 5 have been calcu-

Table 5. Physical parameters for the RRc stars.

Star	[Fe/H] _{ZW}	$M_V(K)$	$\log(L/L_\odot)$	μ_0	D (kpc)
V2	-2.11	0.52	1.700	16.120	16.75
V6	-1.71	0.62	1.664	16.127	16.80
V7	-1.98	0.53	1.698	16.045	16.18
V8	-2.09	0.52	1.702	16.168	17.12
average	-1.97	0.55	1.691	16.115	16.71
σ	± 0.18	± 0.05	± 0.018	± 0.051	± 0.39

lated with a zero point of eq. 4 of 1.061, and are therefore in agreement with a distance modulus of the LMC of 18.5 ± 0.1 (Freedman et al. 2001; van den Marel et al. 2002; Clementini et al. 2003). If the M_V values in Table 5 are compared with the ones obtained by Nemeč (2004) for the same stars after we subtract 0.2 mag from Nemeč's results (labelled as K98 in his Table 14), it can be seen that the two sets of results agree to within ~ 0.02 mag.

For the RRab stars we have used the calibration of Kovács & Walker (2001):

$$M_V(K) = -1.876 \log P - 1.158 A_1 + 0.821 A_3 + K, \quad (5)$$

which has a standard deviation of 0.04 mag.

The zero point of eq. 5, $K = 0.43$, has been calculated by Kinman (2002) using the star RR Lyrae as a calibrator adopting for RR Lyrae the absolute magnitude $M_V = 0.61 \pm 0.10$ mag, as derived by Benedict et al. (2002) using the star parallax measured by the HST. If one adopts $\langle V \rangle = 19.064$ for the RR Lyrae in the LMC and a value of $[\text{Fe}/\text{H}] = -1.5$ (Clementini et al. 2003), then correcting to $[\text{Fe}/\text{H}] = -1.39$ for RR Lyrae (Benedict et al. 2002) one obtains $\langle V \rangle = 19.088$. Hence, the value $K = 0.43$ corresponds to a distance modulus of $19.088 - 0.61 = 18.48$ mag. To make our calculations of the luminosities for the RRab stars consistent with the above values and the distance modulus of 18.5 for the LMC (Freedman et al. 2000), we adopted $K = 0.41$ in the application of eq. 5. The $M_V(K)$ values for the RRab stars are given in Table 4. The average $M_V(K)$ is 0.49 ± 0.06 mag. This result is, within the observational scatter, in good agreement with the mean absolute magnitude found for the RRc stars of 0.55 ± 0.05 mag.

The values of $M_V(K)$ in Tables 4 and 5 were transformed into $\log L/L_\odot$. The bolometric corrections for the average temperatures of RRc and RRab stars were estimated from the calibration for metal poor stars of Montegriffo et al. (1998). We adopted the value $M_{bol}^\odot = 4.75$.

4.3 The effective temperature T_{eff}

The effective temperature of RRc and RRab stars can also be calculated from the Fourier decomposition technique. However, some problems have been identified with the calibrations of RRc stars as we shall discuss below.

For the RRc stars, the calibration of Simon & Clement (1993) can be used:

$$\log T_{\text{eff}} = 3.7746 - 0.1452 \log P + 0.0056 \phi_{31}^{(c)}. \quad (6)$$

For the RRab stars we used the calibration of Jurcsik (1998)

$$\log T_{\text{eff}} = 3.9291 - 0.1112 (V - K)_o - 0.0032 [\text{Fe}/\text{H}] \quad (7)$$

with

$$(V - K)_o = 1.585 + 1.257 P - 0.273 A_1 - 0.234 \phi_{31}^{(s)} + 0.062 \phi_{41}^{(s)}. \quad (8)$$

Eq. 7 has a standard deviation of 0.0018 (Jurcsik 1998), but the uncertainty in $\log T_{\text{eff}}$ is mostly set by the uncertainty in the colour from eq. 8. The error estimate on $\log T_{\text{eff}}$ is 0.003 (Jurcsik 1998).

It has been pointed out by Cacciari et al. (2005) that the temperatures computed from the above equations do not match the colour-temperature relations predicted by the temperature scales of Sekiguchi & Fukugita (2000) or by the evolutionary models of Castelli (1999). This was in fact corroborated by Arellano Ferro et al (2008a) who concluded that the Fourier based temperatures for the RRc need to be reduced by as much as ~ 300 K. In the present paper we explore the colour temperatures from our V, I data and the Vandenberg, Bergbusch & Dowler (2006) HB models, and we perform a comparison with the Fourier temperatures for both RRc and RRab stars.

The value of A_0 in eq. 1 and in Table 3 corresponds in fact to the magnitude-weighted (V) mean magnitude. The values of (I) are listed in Table 6. To deredden the mean magnitudes we have adopted $E(B - V) = 0.018$ (Nemeč 2004) and have calculated the colour ratio $E(B - V)/E(V - I) = 1.58$ from the colour ratios given by Barnes, Evans & Moffett (1978). The values of $(V - I)_o$ for the sample RR Lyrae are also given in Table 6.

To convert the observed $(V - I)_o$ to effective temperatures we have followed Nemeč (2004) in the use of the HB models of Vandenberg, Bergbusch & Dowler (2006) with the colour- $\log T_{\text{eff}}$ relations as described by Vandenberg & Clem (2003). The model with $[\text{Fe}/\text{H}] = -2.012$ and $[\alpha/\text{H}] = 0.3$ was adopted with a polynomial fit of the form:

$$y = A_0 + A_1 x + A_2 x^2 + A_3 x^3 + A_4 x^4 + A_5 x^5 + A_6 x^6 + A_7 x^7 \quad (9)$$

where $y = \log T_{\text{eff}}$, $x = (V - I)_o$ and the coefficients $A_0 = 3.9867$, $A_1 = -0.9506$, $A_2 = +3.5541$, $A_3 = -3.4537$, $A_4 = -26.4992$, $A_5 = +90.9507$, $A_6 = -109.6680$ and $A_7 = +46.7704$. Lower order polynomials do not reproduce the theoretical colour- $\log T_{\text{eff}}$ relations well enough, and the selection of a model with $[\text{Fe}/\text{H}] = -2.310$ does not produce significantly different results. The temperatures obtained from eq. 9 are called $\log T_{\text{eff}}(VI)$.

The values of the Fourier based temperatures, $\log T_{\text{eff}}(\text{Fou})$ (i.e. those obtained from eqs. 6, 7 and 8 for

Table 6. Effective temperatures and radii for the RRc and RRab stars.

Star	(I)	$(V - I)_0$	$\log T_{\text{eff}}$ (Fou)	$\log T_{\text{eff}}$ (VI)	$\log R/R_{\odot}$ (Fou)	$\log R/R_{\odot}$ (VI)	$\log R/R_{\odot}$ (PRZ)
RRc stars							
V2	16.261	0.434	3.852	3.833	0.673	0.708	0.712
V6	16.433	0.364	3.866	3.854	0.632	0.647	0.642
V7	16.232	0.379	3.857	3.850	0.655	0.673	0.692
V8	16.289	0.447	3.854	3.829	0.670	0.717	0.700
RRab stars							
V3	16.188	0.580	3.803	3.793	0.769	0.789	0.747
V4	16.087	0.545	3.797	3.802	0.789	0.780	0.777
V5	16.100	0.545	3.790	3.802	0.795	0.772	0.794
V10	16.023	0.609	3.781	3.786	0.812	0.802	0.815

the RRc and RRab stars respectively) and the VI colour temperatures, $\log T_{\text{eff}}(VI)$, are listed in columns 4 and 5 of Table 6 respectively. These results indicate that for the RRc stars the Fourier based temperatures are on average $\sim 255K$ hotter than the VI colour temperatures, whereas for the RRab stars the agreement is better with the Fourier based temperatures being on average $\sim 40K$ cooler.

The distribution of the RR Lyrae stars in the instability strip is shown in Fig. 3. Two positions have been plotted for each star; for $\log T_{\text{eff}}(Fou)$ (triangles) and $\log T_{\text{eff}}(VI)$ (circles). Three models of the Zero Age Horizontal Branch (ZAHB) from Vandenberg, Bergbusch & Dowler (2006) for $[\text{Fe}/\text{H}] = -1.836$, $[\text{Fe}/\text{H}] = -2.012$ and $[\text{Fe}/\text{H}] = -2.310$ all for $[\alpha/\text{Fe}] = +0.3$ are plotted. The instability strip borders for the fundamental mode and first overtone are also shown (Bono et al. 1995). The distribution of the RRc and the RRab stars resulting from the use of $\log T_{\text{eff}}(Fou)$ values (triangles) looks clumpy. The RRc stars are too blue and the large gap between the RRc and RRab stars is contrary to observational evidence in clusters with larger populations of RR Lyrae stars. For instance, in M3, the distribution of RR Lyrae stars across the instability strip is more even, and some fundamental mode and first overtone pulsator stars share the inter-mode region (Cacciari et al. 2005). The use of the colour temperatures $\log T_{\text{eff}}(VI)$ (circles) produces a larger spread in the RRc stars but not in the RRab stars, which indicates that the Fourier based temperatures for the RRab stars are consistent with the colour temperatures. The colour temperatures distribute the RRc stars more evenly across the instability strip.

4.4 The radius R/R_{\odot}

Given the stellar luminosity and the effective temperature, the stellar radius can be estimated via the expression $\log R/R_{\odot} = [\log(L/L_{\odot}) - 4\log(T_{\text{eff}}/T_{\text{eff}\odot})]/2$. With the Fourier decomposition based values of $\log(L/L_{\odot})$ (or M_V for RRab) and $T_{\text{eff}}(Fou)$, one can derive the stellar radii $\log(R/R_{\odot})(Fou)$. These radii depend fully on the semi-empirical relations and the hydrodynamical models used to calculate the luminosity and the temperature.

An alternative calculation of the radii can be performed

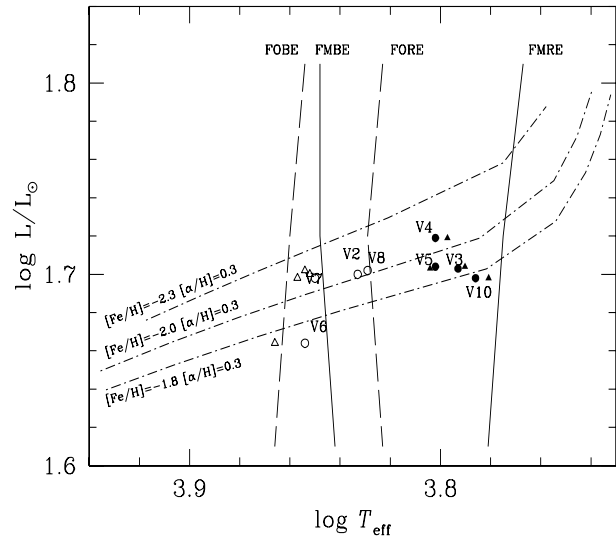


Figure 3. RR Lyrae stars in the HRD for NGC 5053. Solid symbols represent RRab stars and open symbols RRc stars. The triangles were plotted using the Fourier based temperatures, while the circles correspond to colour temperatures calculated from the $(V - I)_0$ index. The vertical boundaries are the fundamental mode (continuous lines) and first overtone (dashed lines) instability strips from Bono et al. (1995) for $0.65 M/M_{\odot}$. The models of the ZAHB (Vandenberg, Bergbusch & Dowler 2006) are shown (dot-dashed lines) for $[\text{Fe}/\text{H}] = -1.836$, -2.012 and -2.310 , all for $[\alpha/\text{Fe}] = +0.3$.

using the colour temperatures $T_{\text{eff}}(VI)$. These radii we shall denote as $\log(R/R_{\odot})(VI)$.

A yet completely independent approach to the RR Lyrae radii determination is through the Period-Radius-Metallicity (PRZ) calibrations of Marconi et al. (2005) which are based on nonlinear convective models (e.g. Bono et al. 2003). Two calibrations are offered; for the first overtone pulsators or RRc stars: $\log R/R_{\odot} = 0.774 + 0.580 \log P - 0.035 \log Z$, and for the fundamental pulsators or RRab stars: $\log R/R_{\odot} = 0.883 + 0.621 \log P - 0.0302 \log Z$. We converted the individual values of $[\text{Fe}/\text{H}]_{\text{ZW}}$ into Z making use of the equation: $\log Z = [\text{Fe}/\text{H}] - 1.70 + \log(0.638 f + 0.362)$, where f is the α -enhancement factor with respect to iron (Salaris et al. 1993) which we adopt as $f = 1$. These radii are listed

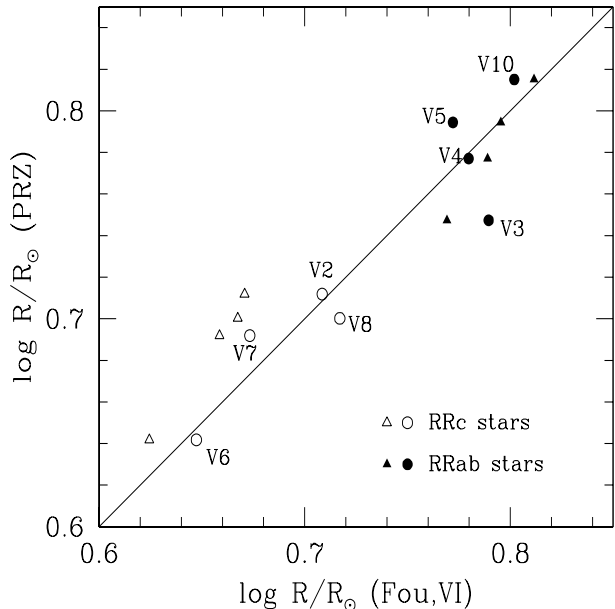


Figure 4. Comparison of radii $\log R/R_{\odot}$ (Fou) (triangles) calculated from the Fourier decomposition parameters $\log(L/L_{\odot})$ and T_{eff} , with those obtained from the Period-Radius-Metallicity calibrations of Marconi *et al.* (2005), $\log R/R_{\odot}$ (PRZ). The radii $\log R/R_{\odot}$ (VI) calculated from the colour temperatures (circles) are in better agreement with $\log R/R_{\odot}$ (PRZ) particularly for the RRc stars. Solid symbols represent RRab stars and open symbols RRc stars. See text in § 4.4 for discussion.

in Table 6 as $\log(R/R_{\odot})$ (PRZ) along with the values of $\log(R/R_{\odot})$ (Fou) and $\log(R/R_{\odot})$ (VI).

A comparison of all of the above estimates of the radii is summarised in Fig. 4 where open triangles indicate that the radii from the Fourier based temperatures, $\log(R/R_{\odot})$ (Fou) for the RRc stars are on average 6% smaller than the PRZ radii $\log(R/R_{\odot})$ (PRZ). For the RRab stars, $\log(R/R_{\odot})$ (Fou) and $\log(R/R_{\odot})$ (PRZ) agree within their uncertainties (solid triangles). On the other hand, the radii from the colour temperatures, $\log(R/R_{\odot})$ (VI), are in agreement with $\log(R/R_{\odot})$ (PRZ) for both the RRc and RRab stars (circles). These results add a word of caution for the temperatures obtained from the calibrations of eq. 6, but confirm that the temperatures for the RRab stars from eqs. 7 and 8 seem consistent with theoretical predictions as pointed out in § 4.3.

4.5 The mass M/M_{\odot}

Fourier-based masses of the RRc stars can be estimated by the calibration of Simon & Clement (1993):

$$\log M/M_{\odot} = 0.52 \log P - 0.11 \phi_{31}^{(c)} + 0.39, \quad (10)$$

and for the RRab stars by the calibration of Jurcsik (1998);

$$\log M/M_{\odot} = 20.884 - 1.754 \log P + 1.477 \log(L/L_{\odot}) - 6.272 \log T_{\text{eff}} + 0.367 [Fe/H]. \quad (11)$$

Cacciari *et al.* (2005) have argued that the masses obtained for RR Lyrae stars from the above relations and the Fourier decomposition of their light curves are not reliable.

Table 7. Masses for the RRc and RRab stars.

Star	M/M_{\odot} (Fou)	M/M_{\odot} (VI)	M/M_{\odot} (Pul)
RRc stars			
V2	0.72	–	0.67
V6	0.70	–	0.69
V7	0.67	–	0.60
V8	0.73	–	0.75
RRab stars			
V3	0.77	0.89	0.86
V4	0.70	0.65	0.68
V5	0.66	0.55	0.59
V10	0.66	0.61	0.62

In order to test these relations in the same way as for the effective temperature, one can compare these masses with those predicted by the fundamental equation of stellar pulsation of van Albada & Baker (1971):

$$\log M/M_{\odot} = 16.907 - 1.47 \log P_F + 1.24 \log(L/L_{\odot}) - 5.12 \log T_{\text{eff}} \quad (12)$$

where P_F is the fundamental period. In order to apply this equation to the first overtone pulsators RRc, their periods were transformed to the fundamental mode by adopting the ratio $P_{1H}/P_F = 0.748$, which is the average ratio for the double mode RR Lyrae stars in M15 (Cox *et al.* 1983). Note that the difference between eq. 12 and the calibration of Jurcsik (1998) in eq. 11 is that the later includes the iron dependence, and therefore a comparison of the two relations is of interest. However, after the discussion in § 4.3 and § 4.4 of the temperature scale, the major concern is how the mass is affected by the chosen temperature scale.

The values of the masses are reported in Table 7. For the RRc stars the Fourier mass M/M_{\odot} (Fou) (eq. 10) and the pulsational mass M/M_{\odot} (Pul) (eq. 12) agree within 10%. Since M/M_{\odot} (Pul) depends on the temperature, we calculated them using the colour temperatures $\log T_{\text{eff}}$ (VI). However, if the Fourier temperatures $\log T_{\text{eff}}$ (Fou) are used instead, the resulting Fourier masses would be more than 20% too small. This also demonstrates that the Fourier temperatures for the RRc (eq. 6) are inaccurate.

For the RRab stars the Fourier mass M/M_{\odot} (Fou) (eq. 11 with Fourier temperature), the colour-temperature based masses M/M_{\odot} (VI) (eq. 11 with colour temperature), and the pulsational mass M/M_{\odot} (Pul) (eq. 12 with colour temperature) are all listed in Table 7. We notice that although the largest differences between the average of colour-temperature based masses (M/M_{\odot} (VI) and M/M_{\odot} (Pul)) minus the Fourier masses (M/M_{\odot} (Fou)) are +14% for V3 and –15% for V5, the average difference including the four RRab stars is only –3%.

In conclusion, the Fourier temperatures for the RRc stars (from eq. 6 of Simon & Clement (1993) seem to be $\sim 250K$ too hot relative to the colour-temperature calibration based on calculations from theoretical models of the HB. This is confirmed by the temperature-dependent Fourier radii and masses when compared with their pulsa-

Table 8. PDM periods of the five known SX Phe stars.

Star	P(days)	
	Nemec et al. (1995)	present work
NC7	0.03683	0.03700
NC11	0.0350	0.03765
NC13	0.03416	0.03396
NC14	0.03925	0.03411
NC15	0.0356	0.03574

tional estimates. This has also been commented by Nemeč (2004) for the RRc temperatures. However, contrary to the suggestion by Cacciari et al. (2005), and despite the larger scatter in the difference between the colour-temperature masses and the Fourier masses compared to the case for the radii, we do not find evidence that the Fourier temperatures for RRab stars from equations 7 and 8 are significantly different from the colour temperatures. The radii and masses based on the Fourier temperatures are comparable to their pulsational estimates.

5 THE BLUE STRAGGLERS AND SX PHOENICIS STARS

5.1 Periods of the SX Phe stars

Four SX Phoenicis (SX Phe) in NGC 5053 were discovered by Nemeč (1989) and a fifth one was later found by Nemeč et al. (1995). Nemeč et al. (1995) determined the main period and discussed the period changes. With our new collection of high quality light curves we believe that we are in a position to revisit these subjects.

The light curves of the SX Phe stars from our data set are displayed in Fig. 5. We have used the Phase Dispersion Minimisation (PDM) approach (Burke et al. 1970; Dworetzky 1983) to first estimate the variability parameter SQ and the period. With the aim of confirming the PDM result and of searching for multiple frequencies we have also used the program PERIOD04 (P4) (Lenz & Breger 2005) on the present data for the five known SX Phe. The final periods found by P4 are listed in column 3 of Table 8. The uncertainties are ~ 0.00001 days. The periods found by Nemeč et al. (1995) are also listed. The differences in period are real due to the intrinsic period variations of the stars and the 20-25 years elapsed between the two data sets. Due to the irregular nature of the variations, likely due to the presence of other undetected frequencies, the light curves in Fig. 5 are not folded with the periods listed in Table 8.

Most likely due to the time distribution of our data set, we found only one frequency in the known SX Phe except for NC13.

For NC13 the period from the PDM method is 0.03421d. The frequencies from the PERIOD04 method are given in Table 9 and correspond to the periods 0.03396d (in agreement with the PDM result), 0.03465d and 0.02680d. The power spectrum corresponding to these periods is shown in Fig. 7 (left). The main frequency and the third one are in the ratio $f_1/f_3 = 0.789$ and therefore they are likely to be the fundamental mode and the first harmonic.

Table 9. Multiple frequencies in the SX Phe star NC13 in NGC 5053.

NC13			
	Frequency (c/d)	Amplitude (mag)	Mode
f_1	29.44274 ± 0.00005	0.044	F
f_2	28.85900 ± 0.00007	0.030	Non radial
f_3	37.31934 ± 0.00012	0.015	$1H$

5.2 Period changes in the SX Phe stars

A first attempt to analyse the period changes in the SX Phe stars in NGC 5053 was made by Nemeč et al. (1995). Since nearly two decades have elapsed between the data employed by these authors and the present data, we have decided to revisit the subject.

The times of maximum light employed by Nemeč et al. (1995) are not explicitly given in their paper and we found that it was inaccurate to try and recover them from their phase diagrams. Instead we opted for inspecting their light curves and estimating the times of maximum. The same procedure was performed on the present light curves in Fig. 5. The times of maximum are reported in Table 10.

In order to build the O-C diagrams of Fig. 6, the periods of Nemeč et al. (1995) and the first time of maximum were adopted as initial ephemerides. Since the pulsational periods are very short and the time elapsed between the two data sets is quite large, the counting of cycles is sometimes uncertain. In Fig. 6 the O-C values that we consider the most likely ones are plotted as solid black circles but alternative values resulting from the addition or subtraction of one cycle are also plotted as open circles. The uncertainty of each individual data point was estimated by Nemeč et al. (1995) to be about 0.1P. However, our estimations of several times of maximum from a single night show a larger dispersion indicated by the vertical error bars in the figure. We believe this is a more conservative and realistic estimate of the individual uncertainties. Brief comments on the period changes of each star are given below

NC7. The O-C diagram for this star suggests that the adopted period is incorrect. However, the amount by which the period is incorrect depends on the cycle counting. In Fig. 6 we show three possibilities. There is no convincing evidence for a secular period change.

NC11. Based on the first two points of the O-C diagram Nemeč et al. (1995) could not argue in favour of a period change. The latest group of O-C data however make a rather convincing case for a period decrease at a rate of -0.101 d/Myr.

NC13. Nemeč et al. (1995) found that the period of this star is increasing. However we find no evidence of an upward parabola on the O-C diagram but rather a downward one implying a period that decreases at a rate of -0.011 d/Myr. Nevertheless the open circles on Fig. 6 show how fragile that conclusion might be. A miscounting of one cycle would imply

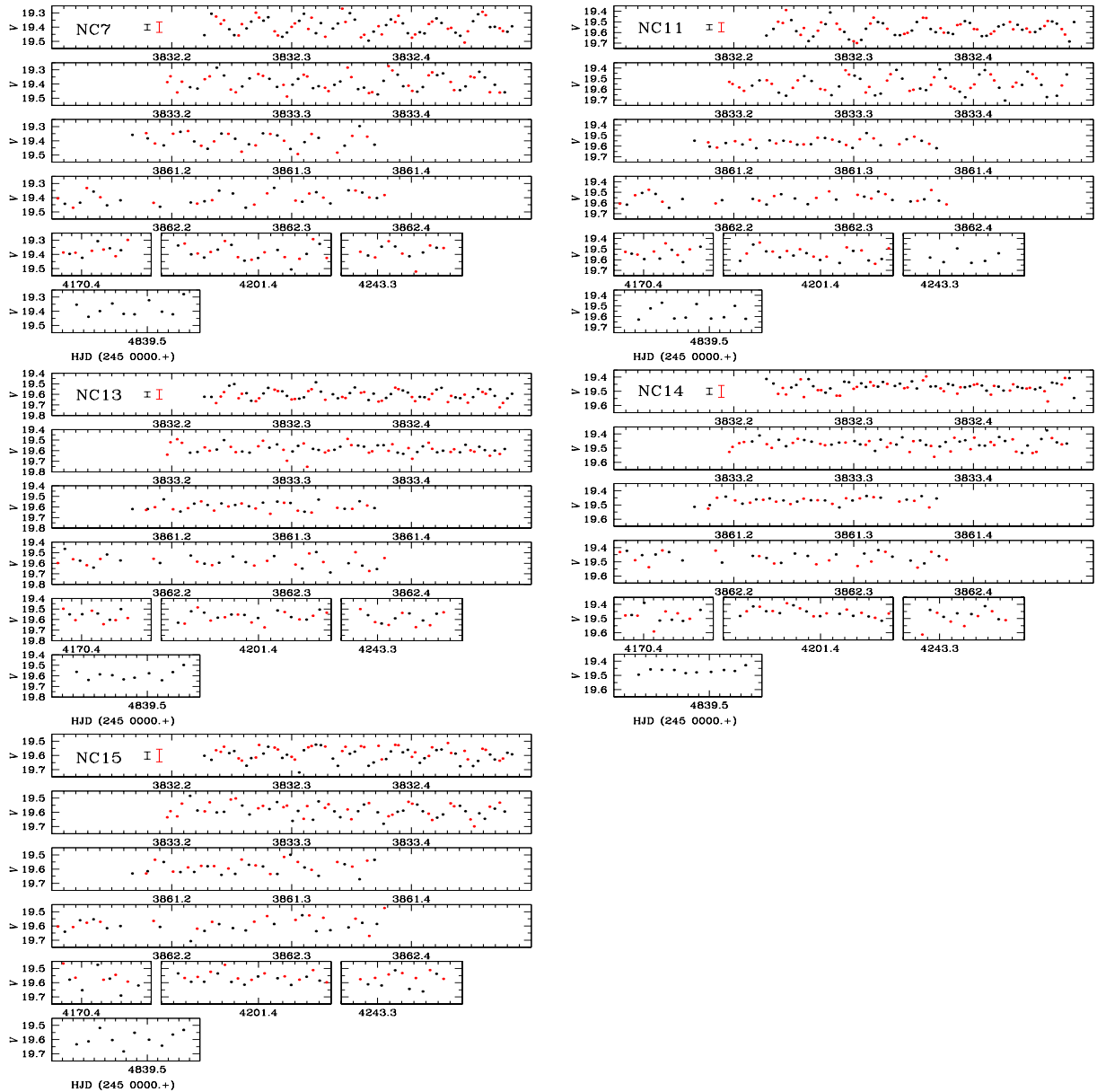


Figure 5. V (black circles) and r (red circles) light curves of the known SX Phe stars in NGC 5053 as obtained in the present work. In order to highlight the variations, the r light curves have been offset in magnitude such that the mean r magnitude matches the mean V magnitude for each star. Mean uncertainties for the V and r data points are plotted at the start of the light curve for clarity.

that the period does not to change at all or changes at a different rate.

NC14. Like NC7, depending upon the cycle counting, three possibilities for the secular behaviour of the period are shown in Fig. 6. If the parabolas are real then the period change rates are -0.008 or -0.0417 d/Myr for the two presented cases. However, given the uncertainties in the times of maximum light, three straight lines of different slopes are also possible.

NC15. Although other possibilities are indicated by the O-C diagram of this star in Fig. 6, it seems that the parabolic fit is a reasonable solution. In that case the rate of period decrease would be -0.084 d/Myr.

All the above period change rates suggested by the parabola fits imply new periods that differ from the

ephemerides by about $\times 10^{-7}$ days or less, and therefore the new periods cannot be confirmed based exclusively on the data of the present paper.

5.3 The Blue Stragglers

There are 28 blue stragglers (BS) reported in NGC 5053, 26 of which are identified by Nemec & Cohen (1989) and Nemec et al. (1995). Five of these BS are the SX Phe variables discussed in § 5.1. Three BS stars were found by Sarajedini & Milone (1995) but their star number 25 is the same as BS25, thus to avoid confusion we shall include Sarajedini & Milone SM26 and SM27 as BS27 and BS28 respectively. We have paid special attention to the identification of each of the BS in our images and our data file collection since some

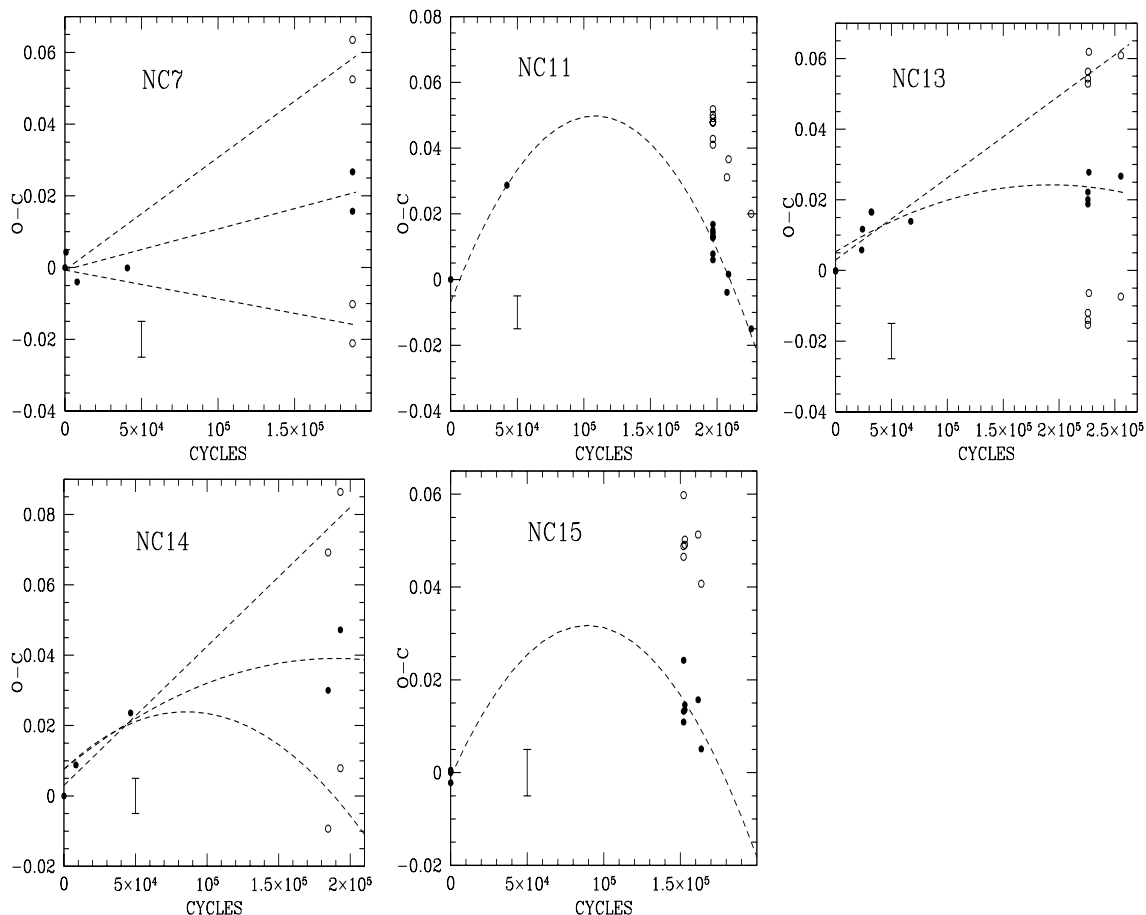


Figure 6. O-C diagrams for the five known SX Phe stars in NGC 5053. Solid circles are the points used to calculate the most suitable parabolic fits, whereas open circles represent alternative values for certain key points by adding or subtracting one cycle. The error bar is the estimate of the uncertainty of each individual point. See text for discussion.

Table 10. Times of maximum light in the SX Phe stars.

NC7 HJD	NC11 HJD	NC13 HJD (2400000. +)	NC14 HJD	NC15 HJD
46914.995	46938.813	46118.153	46587.803	48416.693
46938.828	48416.717	46119.109	46915.903	48416.729
47207.937	53832.289	46915.009	48416.680	48416.798
48416.738	53832.321	46938.790	53833.462	53832.321
53832.311	53832.393	47207.976	54170.401	54243.315
53833.427	53833.259	47218.804		
54839.502	53833.301	53832.251		
	53833.336	53832.321		
	53833.372	53832.425		
	53833.410	53862.329		
	54201.345	54839.535		
	54243.315			
	54839.453			

of them lie in highly crowded regions. We have correctly found the corresponding V , r and I files for 25 of the 28 BS since BS20 lies off the field of our images and BS16 is very near to the image border. BS28 very unfortunately falls on a column of bad pixels on the CCD chip in the I reference image, and therefore we only have V and r light curves.

The identified stars are then highlighted in Fig. 8 as solid yellow circles, open black circles or solid green squares (see caption). The region enclosed by dashed lines in Fig. 8 is the blue straggler region according to Harris (1993) for the cluster NGC 6366, but adapted to the brightness and colour of NGC 5053. 21 of the 25 measured BS stars fall within the

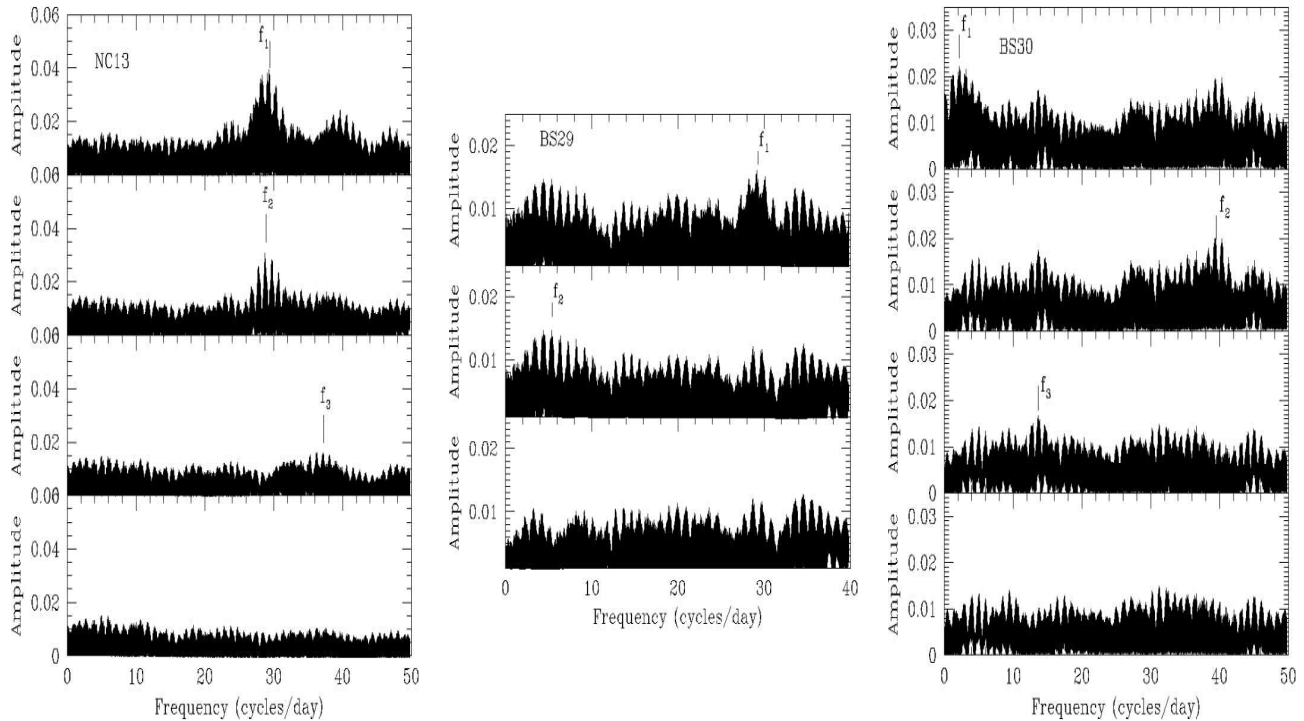


Figure 7. Power spectra of NC13, BS29 and BS30

region confirming their BS nature. The four BS stars that do not fall in the BS region are BS12, BS22, BS23 and BS24 whose $(V - I)$ colour places them on the main sequence turn off region or on the RGB. They are plotted as solid yellow circles for easy identification. Through our dedicated effort towards the identification of these stars, we conclude that these four stars are not likely to be Blue Stragglers.

On the other hand we have found three stars in the BS region not previously identified as BS stars. These are shown as crosses in Fig. 8 and, to continue with the adopted name convention, in what follows we shall refer to them as BS29, BS30 and BS31.

6 SEARCH FOR NEW VARIABLES

All the V light curves of the nearly 6500 stars measured in each of the 151 images available were analysed by the phase dispersion minimisation approach (Burke et al. 1970; Dworetzky 1983). In this analysis the light curve is phased with numerous test periods within a given range. For each period the dispersion parameter SQ is calculated. When SQ is at a minimum, the corresponding period is the best-fit period for that light curve. Bona fide variable stars should have a value of SQ below a certain threshold. Similar analysis has been used and described in detail in previous papers (e.g. Arellano Ferro et al. 2008a;b, 2006). In Fig. 9 the distribution of the SQ parameter for the whole sample of stars is shown. As expected the RR Lyrae stars (solid blue circles) have the smallest values of SQ . However it should be noted that the five known SX Phe stars (solid green circles) all have large values of SQ despite their variability. Likewise, the BS stars (solid turquoise circles) present large values of SQ , and hence their possible variability cannot be ruled out

by the SQ method. We will analyse the BS stars in § 6.1. The V light curves for all stars with $SQ < 0.35$ were visually inspected (black crosses) and only two are convincing variables; NV1 (solid red circle) and BS4. Their periodicities will be discussed below.

Fig. 10 shows the logarithm of the standard deviation of the mean ($\log \sigma$) as a function of mean magnitude. Stars with large dispersion for a given magnitude are good candidates to be variable. This figure, in combination with Fig. 9 can be used to identify new variables. In Figs. 9 and 10 we also plot the RR Lyrae stars, SX Phe stars, BS stars and the new variables that will be discussed in detail in the forthcoming sections.

6.1 Variability among BS stars

Apart from the 5 stars identified as SX Phe among the BS stars, Nemeč et al. (1995) suspected variability in the stars BS12, BS21 and BS25. We explored each BS star light curve in our collection and found clear indications of variability in some of them. In what follows we will discuss their periodicities and in Table 11 we summarise the properties of the whole collection of confirmed and new BS stars. It should be stressed however, that variables in the BS region often show multiple frequencies and small amplitudes, e.g. SX Phe stars, and that our light curve sampling is far from ideal to establish complicated frequency patterns; although the time span is three years, the inter-run gaps are large and hence the window function is complicated. This problem was also a limitation of the period determination by Nemeč et al. (1995), hence in depth study of the frequency content of the variable BS stars, including the known SX Phe stars, long multisite observing campaigns would be required. Thus we

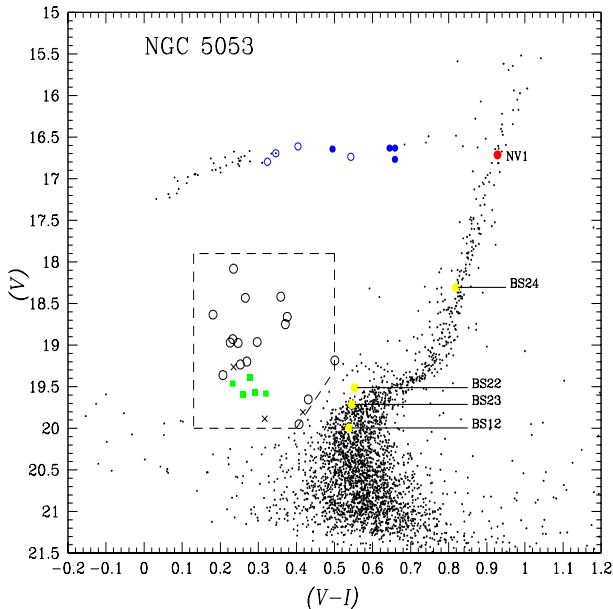


Figure 8. Variable stars in the colour-magnitude plane of NGC 5053. Solid blue circles represent RRAb stars and open blue circles represent RRC stars. The region enclosed by dashed lines is the blue straggler region in NGC 6366 according to Harris (1993) but adapted to the corresponding brightness and colour of NGC 5053. Open black circles are previously known BS stars and crosses are newly identified BS stars BS29, BS30 and BS31. Solid green squares correspond to the five SX Phe stars known to Nemeč et al. (1995). The solid yellow circles correspond to stars BS12, BS22, BS23, BS24 previously identified as BS stars which we do not confirm as such. A new RGV, NV1, is shown as a solid red circle.

aim to find/confirm the variability among the BS stars and to determine the main periodicity, although in a few cases, we are able to detect a second frequency.

The BS stars have mean V magnitudes between 18 and 20. In this range the magnitude errors are between 0.01 and 0.04 mag (see Fig. 10). Keeping this in mind, we have classified the BS stars as variable, suspect variable and non-variable. We confirm the variability of BS25 suspected by Nemeč et al. (1995), and we also find variability in BS4, BS5, BS19, BS28, and in the newly discovered BS stars BS29 and BS30. In Fig. 10, known and new BS stars are shown as solid turquoise circles except for the variable ones that are labelled and represented by solid yellow circles. We describe below our attempts to find their periodicities.

Our approach to determining the periodicities of the BS stars involves a PDM analysis of the light curve to find a first estimate of the period. Then P4 was run as a confirmation and to search for other frequencies. Since the period range in 149 SX Phe stars in Galactic globular clusters is between 0.03 and 0.14d (Rodríguez & López-González 2000), we started searching in this range. However, for specific cases shorter or longer periods were explored. We address each star individually in the following paragraphs.

6.1.1 Periodicities in variable BS stars

The light curves of the variable BS stars are shown in Fig. 11.

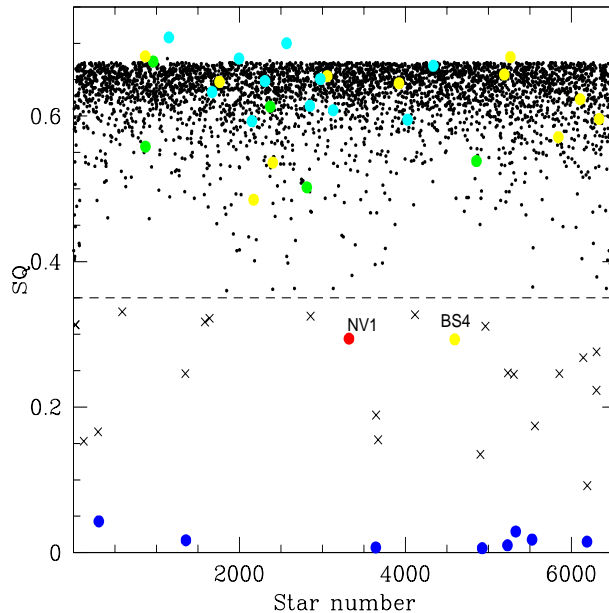


Figure 9. SQ parameter distribution for all stars with V light curves in the field of NGC 5053. Light curves for stars below the $SQ = 0.35$ dashed line were individually explored, and only two were classified as variables; NV1 (solid red circle) and BS4. Solid blue circles correspond to the known RR Lyrae stars. Solid green circles are the five known SX Phe stars. Solid turquoise circles are non-variable BS stars. Solid yellow circles are the variable BS stars.

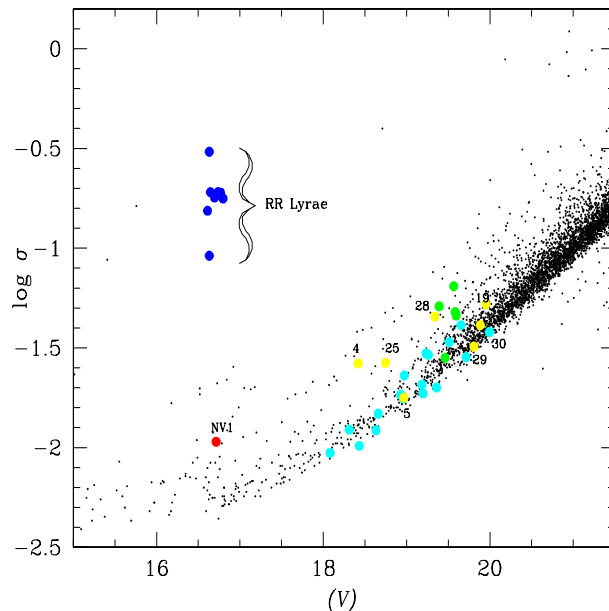


Figure 10. Logarithm of the standard deviation of the mean ($\log \sigma$) as a function of the mean magnitude (V). Stars above the main cluster of points are good candidate variables, although small amplitude variability may be found among stars with small $\log \sigma$. Solid blue circles are RR Lyrae stars. Solid green circles are the five known SX Phe stars. Solid turquoise circles are non-variable BS stars and labelled solid yellow circles are variable BS stars. The new RGB variable is shown as a solid red circle.

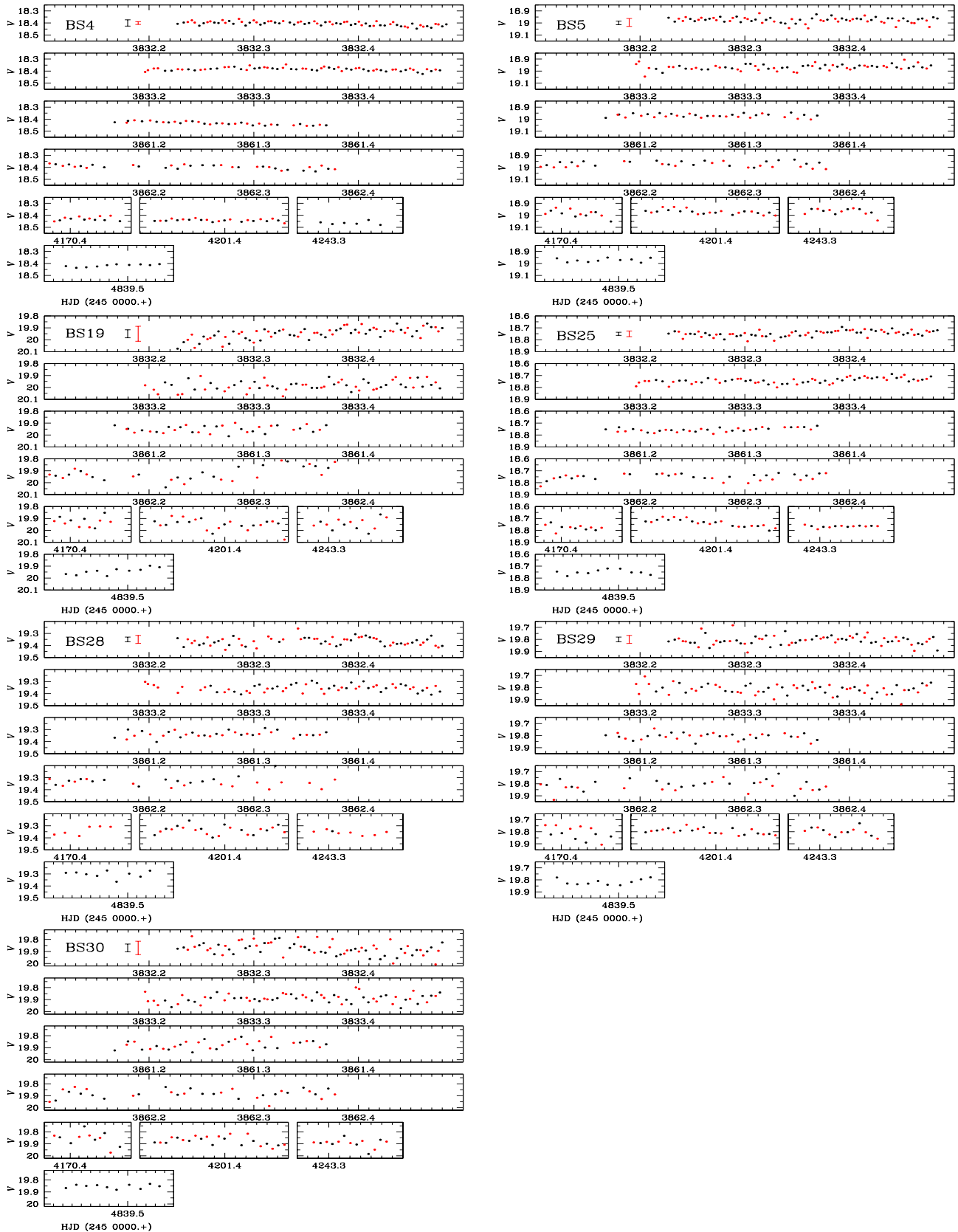


Figure 11. *V* (black circles) and *r* (red circles) light curves of the variable BS stars in NGC 5053 as obtained in the present work. In order to highlight the variations, the *r* light curves have been offset in magnitude such that the mean *r* magnitude matches the mean *V* magnitude for each star. Mean uncertainties for *V* and *r* data points are plotted at the start of the light curve for clarity. The vertical scale is the same for all stars.

Table 11. Blue stragglers in NGC 5053. For known SX Phe we retained the nomenclature NC after Nemec et al. (1995). New BS and not confirmed BS stars are also listed.

Star	(<i>V</i>) (mag.)	Variable	<i>P</i> (days)	Type	Notes
BS1	18.082	no			
BS2	18.432	no			
BS3	18.660	no			
BS4	18.418	yes	0.52382	?	NV
BS5	18.969	yes	0.03847	SX Phe	NV
BS6	18.633	no			
NC7	19.391	yes	0.03700	SX Phe	known
BS8	19.233	no			
BS9	18.975	no			
BS10	18.963	no			
NC11	19.566	yes	0.03765	SX Phe	known
BS12	19.995	no			nBS
NC13	19.583	yes	0.03396	SX Phe	known
NC14	19.463	yes	0.03411	SX Phe	known
NC15	19.596	yes	0.03574	SX Phe	known
BS16					not included
BS17	19.361	no			
BS18	19.652	no			
BS19	19.951	yes	0.02929	SX Phe?	NV
BS20					not included
BS21	18.928	no			
BS22	19.512	yes?	0.07725	?	nBS
BS23	19.714	yes?	0.12102	?	nBS
BS24	18.307	no			nBS
BS25	18.748	yes	0.04521	SX Phe	NV
BS26	19.184	no			
BS27	19.808	no			SM26
BS28	19.339	yes	0.04547	SX Phe	SM27, NV
BS29	19.808	yes	0.03411	SX Phe	NBS, NV
BS30	19.885	yes	0.02535	SX Phe	NBS, NV
BS31	19.263	yes?	0.05105	SX Phe?	NBS

Notes: NV: new variable, nBS: not a Blue Straggler, NBS: new Blue Stragglers, SM26 & SM27 discovered by Sarejedini & Milone (1995)

BS4. No clear short periods are visible in the light curve and instead we find long term mean magnitude changes. Two PDM periods are found; 0.07014d and 0.52382d. While the first period is typical of an SX Phe star, it does not produce a coherent folded light curve. On the other hand P4 finds a period of 1.10354d which is nearly twice the longer PDM period. In Fig. 12 the *V, r, I* light curves are phased with the ephemerides $HJD_{\max}=245\ 3833.3057+0.52382E$, although the period 1.10354d cannot be ruled out.

BS5. Variations with a characteristic time of the order of 0.1d are visible in the light curve. In fact the light curve is similar to that of the SX Phe star NC14 in Fig. 5. The PDM period is 0.12659d while P4 finds 0.02308, 0.03847 and 0.12678d. One cannot *a priori* favour any one of these periods, although we note that if the star is indeed a SX Phe, as suggested by its position on the CMD, then the period 0.03847d would be the most consistent with the expectation from the PL relationship for SX Phe (see § 6.2).

BS19. The light variation is very evident. The PDM period is 0.07877d. P4 finds a prominent peak at 0.60889d, and after prewhitening, a peak at 0.02929d appears. This

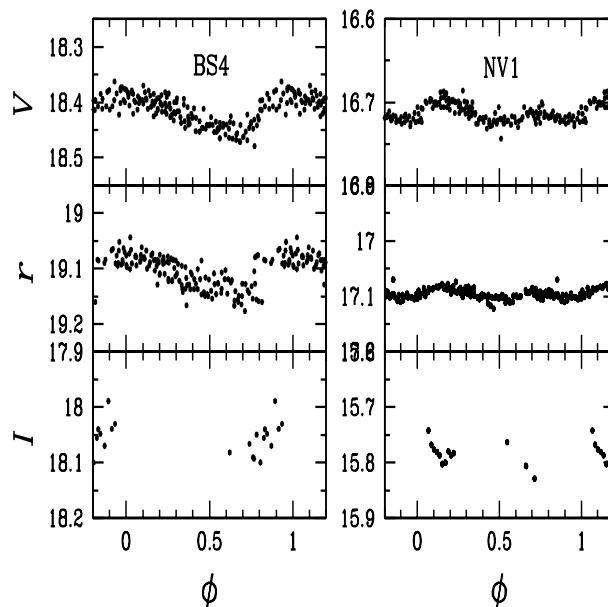


Figure 12. Folded *V, r, I* light curves of two newly identified variables.

is a similar case to that of BS4 but the phasing with the longer period 0.60889d does not produce a convincing light curve. If the short period is confirmed with more data then the star might be an SX Phe star.

BS25. This star is in a crowded region but it can be well measured by our difference imaging technique. In fact, the average magnitude uncertainties for this $V=18.7$ mag star are among the smallest for the BS stars; 0.013 and 0.024 in *V* and *r* respectively. Therefore the variations, although of small amplitude, are likely to be real and we carried out a search for the periodicity. The PDM period is 0.17224 while P4 finds a substantial peak at 0.20821d and a secondary peak at 0.04521. The later period would be consistent with the first harmonic of a SX Phe star of the brightness of BS25, according to the SX Phe *PL* relation (see § 6.2).

BS28. The light curve shows signs of variability. Some epochs are missing because the star falls near a bad pixel column in the chip and then in some images the photometry is unreliable. The PDM analysis indicates a period of 0.17425d. P4 finds two major peaks at 0.20408d and 0.04547d. The star is probably an SX Phe.

BS29. Clear signs of variability are seen in the light curve. The PDM period is 0.142412d. P4 finds a strong peak at 0.034110d which is nearly one fourth of the PDM period. Prewhitening the main period one finds 0.18477d (see Fig. 7). It is likely that these two frequencies are real. The star is a new BS star and likely an SX Phe.

BS30. Clear signs of variability are also seen in the light curve of this star. The PDM period is 0.07290d. P4 finds a strong and substantial peak at 0.45045d ($A=0.0215$ mag). Prewhitening the major frequency one finds 0.02535d. The period 0.45045d does not fold the light curve at all and therefore it must be a spurious alias. The shorter period is likely to be correct. This is a new BS star and very likely an SX Phe.

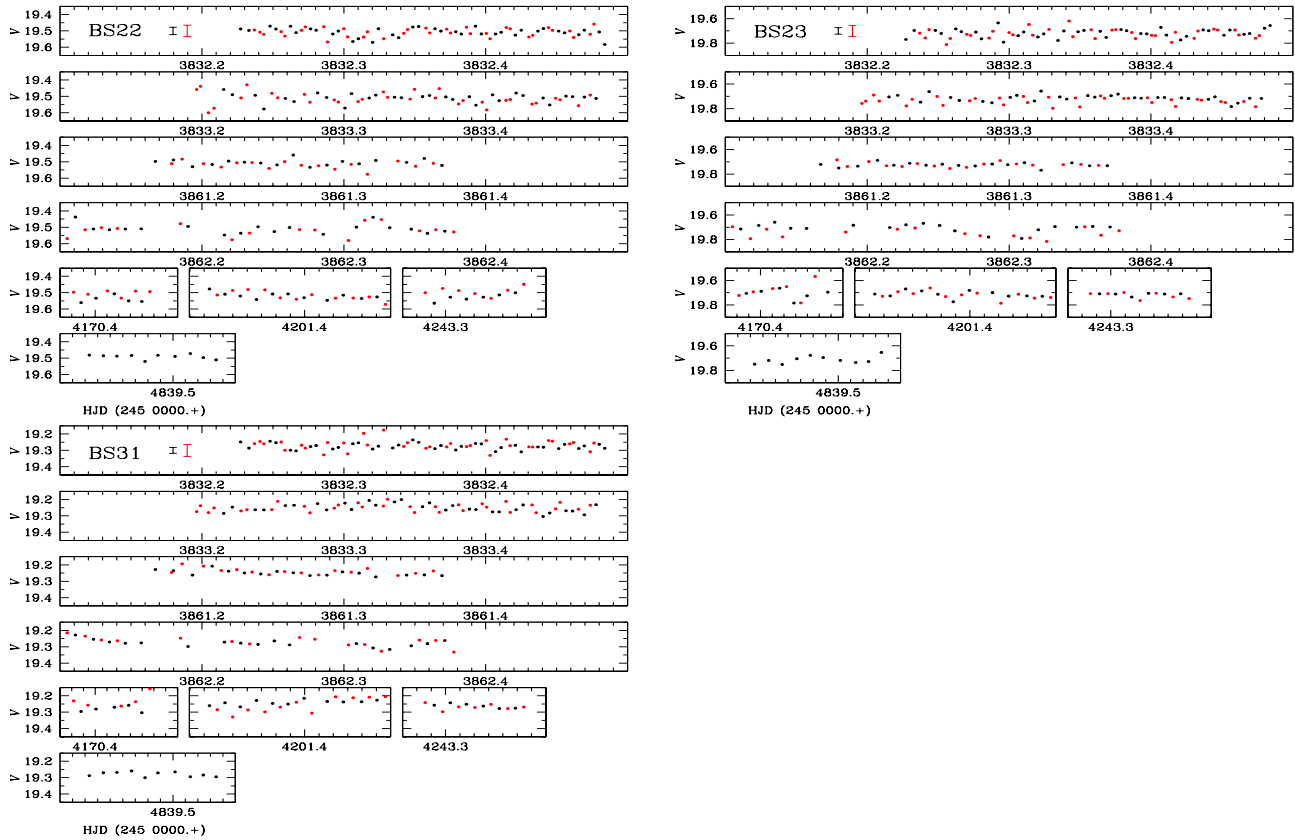


Figure 13. V (black circles) and r (red circles) light curve of suspect variable BS stars in NGC 5053 as obtained in the present work. In order to highlight the variations, the r light curves have been offset in magnitude such that the mean r magnitude matches the mean V magnitude for each star. Mean uncertainties for V and r data points are plotted at the start of the light curve for clarity.

6.1.2 Periodicities in suspect variable BS stars

The light curves of the suspect variable BS stars in Fig. 13.

BS22. Considering the average magnitude uncertainties indicated in the figure, mild indications of variability are seen in light curve, especially when the V and r data are combined. We decided to perform a period search in the V data. The PDM period is 0.15580d. P4 finds 0.07725d and a competing period is 0.16155d. As for the other BS stars, the removal of the main frequency leaves substantial signal in the power spectrum, suggesting the presence of other frequencies which we are unable to determine with the available data. The star is not a BS star as it sits on the turn off region on its way to the RGB. Its variability will require confirmation with a more appropriate data set.

BS23. Similar to BS22, the variations in BS23 are mild. The PDM period is 0.12102d. P4 shows three competing peaks in the main structure of the power spectrum at periods 0.12561, 0.11365 and 0.10287d. The star is not a BS star as it lies in the turn off region (see Fig. 8).

BS31. The mean magnitude uncertainties for this star are 0.018 and 0.036 mag in V and r respectively, which implies that the observed variations are probably real. The PDM period is 0.02574d, which is too short for an SX Phe star. P4 indicates two competing periods of 0.04556d and 0.05105d. The later is about twice the PDM period and hence the most likely period. If the variation and period are confirmed then this star might be an SX Phe.

6.2 The SX Phe PL relation and the distance to NGC 5053

It is known that SX Phe stars follow a tight relation between their fundamental mode, first overtone periods and their luminosity (McNamara 1995). Due to the mixture of modes, the Period-Luminosity (PL) relation is difficult to determine. Of particular relevance to the present work is the calibration that Jeon et al. (2004) calculated for seven SX Phe in NGC 5466; $M_V = -3.25(\pm 0.46) \log P - 1.30(\pm 0.06)$ ($\sigma = 0.04$), because the distance and iron content of NGC 5466 (16.06 \pm 0.09 kpc and -1.91 ± 0.19 ; Arellano Ferro et al. 2008a) are almost identical to our values determined for NGC 5053 (16.75 \pm 0.39 kpc and -1.97 ± 0.16). A PL dependence on $[\text{Fe}/\text{H}]$ has been proposed by Nemeč et al. (1994) of the form: $M_V = -2.56(\pm 0.54) \log P + 0.36 + 0.32[\text{Fe}/\text{H}]$.

In Fig. 14 we have plotted the logarithm of the period (column 4 Table 11) vs. the mean magnitude (V) (column 2 Table 11) for the 5 known SX Phe stars and the BS stars identified as SX Phe stars in § 6.1. The calibrations of Jeon et al. (2004) and Nemeč et al. (1994) are shown as continuous and dashed lines respectively and have been scaled to the case of NGC 5053 using a distance modulus of 16.125 and $E(B - V) = 0.018$. It can be seen that the SX Phe stars in NGC 5053 follow the above two relations. The most discordant stars would seem to be BS5 and BS25. However, their periods found in § 6.1 seem to correspond to the first overtone, as suggested by the first overtone calibration of

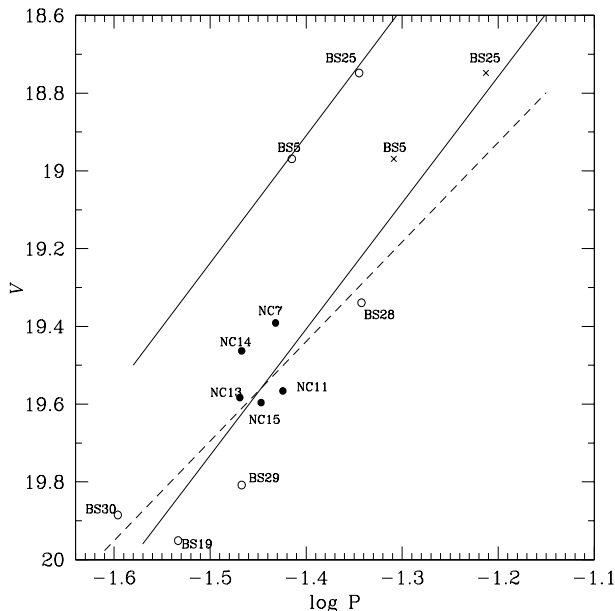


Figure 14. Period-Luminosity relation for the SX Phe stars in NGC 5053. Filled circles represent the known SX Phe stars. Open circles represent the newly identified SX Phe stars among the BS stars. Two positions are shown for BS5 and BS25 for the first overtone period (open circles) and the fundamental period (crosses). The two continuous lines correspond to the first overtone and fundamental mode relations of Jeon et al. (2004) and the dashed line represents the relation of Nemeč et al. (1994).

Jeon et al. (1994). Their periods can be converted to the fundamental mode via the ratio $P_{1H}/P_F = 0.783$ (Jeon et al. 2004), and then the stars also seem to follow the fundamental mode relation (crosses in Fig. 14).

The distribution of the BS stars along the PL relations for SX Phe stars confirms their SX Phe nature. Since the period for the SX Phe stars in NGC 5466 is better determined than for the SX Phe stars in NGC 5053, rather than attempting an independent calibration of the PL relation, the SX Phe (known and newly discovered) can be used to estimate the distance to NGC 5053.

The application of the PL relations of Jeon et al. (2004) and of Nemeč et al. (1994) lead to the average distances of 16.36 ± 0.85 and 16.08 ± 0.98 kpc respectively. Although these determinations of the distance cannot compete in precision with the determination from the RR Lyrae stars, it is rewarding to find that the agreement is good to within the uncertainties.

6.3 Other new variables

In Fig. 10 it can be observed that above the main stream there are numerous points which may be variables. An exploration of all of the corresponding data files up to $V \sim 20$ shows that often the large sigmas are produced by a few occasional spurious measurements, particularly in stars near to the border of our images, or near to saturated or to authentic variable stars, and are not due to intrinsic variability. However, we find one star suspected of real variations as addressed below.

NV1. On the CDM this star is on the RGB. Its PDM period of 0.66578d phases the variations well in all filters (Fig. 12). No evidence of more frequencies was found with the data on hand. P4 suggests two peaks at 1.69426d and 0.63921d, none of which phase the light curve as well as the PDM period.

In Fig. 15 we display a finding chart for the eight RR Lyrae stars studied, the five previously known SX Phe stars, the variable BS stars, the three new BS stars and the new variable NV1.

7 DISCUSSION

7.1 On the distance to NGC 5053

To determine the distance to the cluster we have calculated the distance modulus ($A_0 - M_V$) for each RR Lyrae star, using the absolute magnitudes $M_V(K)$ given in Tables 5 and 4, and the mean magnitudes A_0 from Table 3. We used the extinction ratio $R=3.2$ and the value of $E(B - V) = 0.018$ was adopted from Nemeč (2004).

We find mean true distance moduli of 16.12 ± 0.05 and 16.12 ± 0.03 , which correspond to distances of 16.71 ± 0.39 kpc and 16.75 ± 0.26 kpc for the RRc and RRab stars respectively. The uncertainties quoted for these values correspond to the standard deviation of the mean. These values of the distance are consistent with the mean luminosity of the RR Lyrae stars in the LMC $V_o = 19.064 \pm 0.064$ (Clementini et al. 2003) and a distance modulus of 18.5 ± 0.1 mag for the LMC (Freedman et al. 2001; van den Marel et al. 2002; Clementini et al. 2003).

In his catalogue of parameters of globular clusters, Harris (1996) lists a distance of 16.4 kpc for NGC 5053, which comes from the assumption of $V(\text{HB})=16.65$ (Sarajedini & Milone 1995), $[\text{Fe}/\text{H}]=-2.29$, $R=3.0$, $E(B - V) = 0.04$ and the relation $M_V = 0.15[\text{Fe}/\text{H}] + 0.80$. His calculation is mostly sensitive to the values of $[\text{Fe}/\text{H}]$ and $E(B - V)$. If the calculation is repeated with the value $[\text{Fe}/\text{H}]=-1.97$, and depending upon the assumed value of $E(B - V)$ between 0.018 and 0.04 mag, one obtains a distance in the range 16.04 to 16.53 kpc. No significant differences are found if a reasonably different M_V - $[\text{Fe}/\text{H}]$ relation is used.

The Fourier results for the distance are independent of the iron abundances however, they seem to support the estimate made using low metallicity.

7.2 On the age of NGC 5053

We have estimated the age of the cluster by a direct comparison of the cluster's CMD with the theoretical isochrones of Vandenberg, Bergbusch & Dowler (2006) as shown in Fig. 16. To properly align the theoretical isochrones with the observed distribution of stars, we aligned the most blue point on the isochrones with the Turn Off (TO) point. Indeed, the main source of uncertainty in this procedure is in the location of the TO point. In fact, Rosenberg et al. (1999) report that the TO point of NGC 5053 is at $V = 20.00 \pm 0.06$ and $(V - I) = 0.545 \pm 0.004$. This TO point is shown in Fig. 16 as a solid white circle and indicates that the best fit model is for an age of ~ 16 Gyrs, as shown in the bottom panel. The age seems much too large when compared to the most

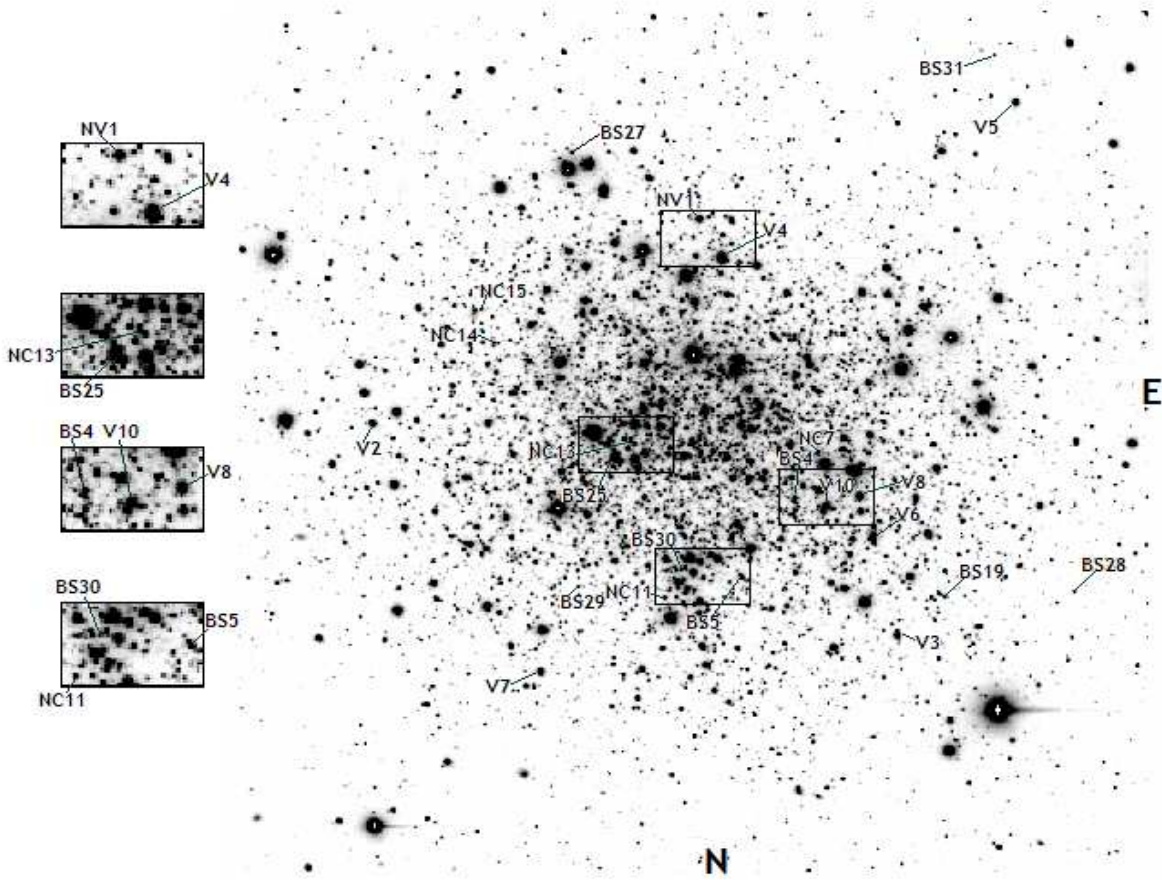


Figure 15. V image of NGC 5053 obtained at the Indian Astrophysical Observatory at Hanle, India. The size is approximately 11×11 arcmin². All RR Lyrae stars are identified with prefix V, Blue Stragglers with prefix BS, and the five previously known SX Phe stars with prefix NC. The two BS stars found by Sarajedini & Milone (1995) are BS27 and BS28. The three new BS stars found in this work are BS29, BS30 and BS31. The rest of the Blue Stragglers are clearly identified by Nemeč & Cohen (1989).

recent differential calculations of globular cluster ages (as we shall see below) which further implies that the adopted TO point is too red.

We have attempted our own estimate of the location of the TO point. We adopted $V = 20.0$, but for the $(V - I)$ value we proceeded as follows; the mean uncertainties in our photometry at $V = 20.0$ and $I = 19.5$ are 0.04 and 0.05 mag respectively, and hence the uncertainty in $(V - I)$ is ~ 0.06 mag, which is represented by the horizontal error bars shown in Fig. 16. To allow for this uncertainty in the colour, we have shifted the TO point from the bluest point of the bulk of stars at $V = 20.0$, by 0.06 mag redwards. In the top panel of Fig. 16 we have fixed the isochrones on this new TO point as we did in the bottom panel. The best fit of the RGB would be for a model of age between 12 and 14 Gyrs. The best fits for 12 Gyrs and 14 Gyrs would be obtained for shifts of the TO from the bluest point of 0.05 and 0.09 mag respectively. A linear interpolation in between these two models for 0.06 mag gives an age of 12.5 Gyrs. The uncertainty attached to this estimate is related to the uncertainty in the location of the TO point due to uncertainties in the photometry. Shifting the TO point ± 0.03 mag would correspond to an uncertainty of about ± 2.0 Gyrs in the age estimation.

A differential version of the vertical and horizontal

methods for globular cluster age determination for a family of Galactic globular clusters can be found in the work of Rosenberg et al. (1999). NGC 5053 is included in the cluster sample used by these authors who estimate an average age for the cluster of -0.9 ± 0.07 Gyrs relative to the absolute age of a group of coeval clusters assumed to have an age of 13.2 Gyrs as in Carretta et al. (2000). In other words, their estimate for the age of NGC 5053 is 12.3 ± 0.7 Gyrs. These authors consider NGC 5053 to be a member of the coeval group.

The CMD in Fig. 16 is comparable to the CMD of the cluster published by Rosenberg et al. (2000), which is to be expected since we have used the same set of standard stars. The Rosenberg et al. (2000) diagram was used by Rosenberg et al. (1999) to estimate the age of the cluster. The horizontal fiducial lines in Fig. 16 from the bottom upwards correspond to the TO point, the fiducial point on the RGB 2.5 mag above the TO point ($RGB_{2.5}$), and the level of the HB respectively. We have estimated the age sensitive vertical and horizontal parameters $\Delta V_{TO}^{HB} = TO - HB = 3.35 \pm 0.05$ mag and $\delta(V - I)_{2.5} = RGB_{2.5} - TO = 0.359 \pm 0.050$ mag, that can be compared with those estimated by Rosenberg et al. (1999) as 3.30 ± 0.08 and 0.310 ± 0.007 respectively. It is clear that vertically our results agree well and hence similar

ages would be found. However, due to the substantially different horizontal position of the TO point, a large difference is exhibited between the values of the $\delta(V-I)_{2.5}$ parameter. Despite this discrepancy, our estimate agrees well with their horizontal estimate of the age of 12.6 ± 0.5 Gyrs. This is probably due to the fact that, despite Rosenberg et al.'s (1999) absolute estimation of the mean age for the group of coeval clusters from the horizontal parameter and a comparison with the models of Straniero et al. (1997) and Vandenberg et al. (1990) of 13.1 and 16.4 Gyrs respectively, they adopt an age for the coeval group of 13.2 Gyrs, and then estimate individual cluster ages differentially. Our estimate for the age of NGC 5053 agrees well within the uncertainties with the final average age given by Rosenberg et al. (1999).

Another age estimate for NGC 5053 obtained by employing a differential approach is that of Salaris & Weiss (2002) who found an age of 10.8 ± 0.9 Gyrs. The most recent differential age calculation for 64 galactic globular clusters was made by Marín-Franch et al. (2009) using four sets of stellar evolution libraries. These authors find an average relative age $A_{NGC\ 5053}/A_{bulk} = 0.96 \pm 0.04$, and using the models of Dotter et al. (2007), they calculated a mean absolute age for the low metallicity clusters of 12.8 ± 0.17 Gyrs, from which one can calculate an age of 12.29 ± 0.17 Gyrs for NGC 5053.

There is reasonable agreement between our result of 12.5 ± 2.0 Gyrs with the three independent and more accurate differential age estimates of 12.3 ± 0.7 Gyrs (Rosenberg et al. 1999), 10.8 ± 0.9 Gyrs (Salaris & Weiss 2002) and 12.29 ± 0.17 Gyrs (Marín-Franch et al. 2009).

8 CONCLUSIONS

The technique of difference imaging has proven to be a powerful tool in providing accurate photometry down to about $V = 20$ mag and in finding new variables. In this paper we report the discovery of five SX Phe stars among the BS stars, two of which are new BS stars, and one new red semiregular variable.

Physical parameters of astrophysical relevance such as: $\log(L/L_\odot)$, $\log T_{\text{eff}}$, M_V , R/R_\odot , M/M_\odot and $[\text{Fe}/\text{H}]$, have been derived for the RR Lyrae stars in NGC 5053 using the Fourier decomposition of their V light curves. Special attention has been paid to the calibration of these parameters onto widely accepted scales. It has been found that T_{eff} for the RRc stars from the calibration of Simon & Clement (1993) cannot be reconciled with the theoretical predictions for the boundaries of the instability strip. However, the Fourier temperatures for RRab stars from the calibration of Jurcsik (1998) agree well with the colour temperatures, and they imply radii and masses comparable to those derived from pulsational models.

The average iron abundance $[\text{Fe}/\text{H}] = -1.97 \pm 0.16$ is found from the RRab and RRc stars. This value may appear too large for a cluster often considered the most metal deficient in the Galactic halo. However, this value is in good agreement, within the uncertainties, with the most recent accurate estimates from spectroscopic data.

A distance of 16.7 ± 0.3 kpc is found from the Fourier approach to the determination of M_V for the RR Lyrae stars. This value is in agreement, within uncertainties, with pre-

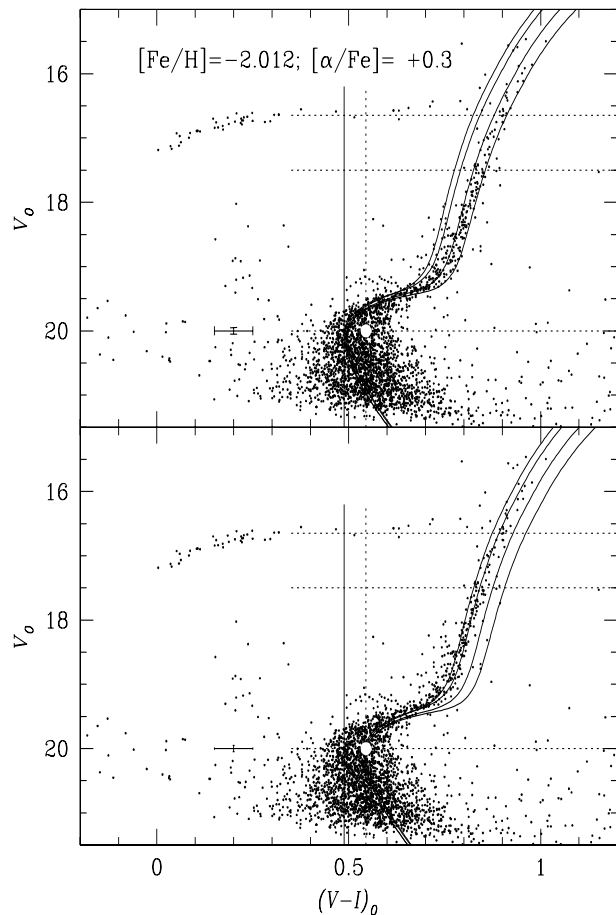


Figure 16. Isochrones from models with $[\text{Fe}/\text{H}] = -2.012$ and $[\alpha/\text{Fe}] = 0.3$ of Vandenberg, Bergbusch & Dowler (2006). The ages of the isochrones are identified at the RGB from right to left as 12, 14, 16 and 18 Gyrs. The bottom panel shows the models aligned with the turn off point (TO) of Rosenberg et al. (2000) (solid white circle). In the top panel the models are aligned with the TO point calculated in the present paper. The error bars correspond to the mean uncertainties of the V and I photometry at $V = 20.0$ mag and $I = 19.5$ mag. See text for discussion.

dictions from the M_V - $[\text{Fe}/\text{H}]$ relation for values of $[\text{Fe}/\text{H}] \sim -2.0$.

We report five new SX Phe stars and show that they follow the period luminosity relationship of SX Phe stars in NGC 5466, a cluster very similar in age and metallicity to NGC 5053. If the PL calibration is applied to the SX Phe in NGC 5053, then the estimated distance is found in good agreement with the distance from the RR Lyrae stars.

Our $(V-I)$ CMD and the isochrones of Vandenberg, Bergbusch & Dowler (2006) indicate an age of 12.5 ± 2.0 Gyrs for the cluster, which is in good agreement with independent differential age estimations.

ACKNOWLEDGMENTS

We are grateful to the support astronomers of IAO, at Hanle and CREST (Hosakote), for their efficient help while acquiring the data and to the referee for the detailed revision and very useful suggestions. The help of Victoria Rojas with the

production of Fig. 15 is acknowledged with gratitude. We acknowledge support from the DST-CONACYT collaboration project and the DGAPA-UNAM grant through project IN114309 at several stages of the work. AAF is grateful to the IIA for their warm hospitality. DMB is thankful to the Instituto de Astronomía of the Universidad Nacional Autónoma de México for their hospitality. This work has made a large use of the SIMBAD and ADS services, for which we are thankful.

REFERENCES

- Alard C., 2000, *A&AS*, 144, 363
 Alard C., Lupton R.H., 1998, *ApJ*, 503, 325
 Arellano Ferro A., Arévalo M. J., Lázaro C., Rey M., Bramich D. M., Giridhar S., 2004, *RevMexAA*, 40, 209
 Arellano Ferro, A., Rojas López, V, Giridhar, S., Bramich, D.M., 2008a, *MNRAS*, 384, 1444
 Arellano Ferro, A., Giridhar, S., Rojas López, V, Figuera, R., Bramich, D.M., Rosenzweig, P., 2008b, *RevMexAA*, 44, 365
 Armandroff, T.E., Da Costa, G.S., Zinn, R.J., 1992, *AJ*, 104, 164
 Barnes, T. G., Evans, D. S., Moffett, T. J., 1978, *MNRAS*, 183, 285
 Bell, R.A., Gustafsson, B., 1983, *MNRAS*, 204, 249
 Benedict G. F., McArthur, B. E., Fredrick, L. W., et al. 2002, *ApJ*, 123, 473
 Bono G., Caputo F., Castellani V., Marconi M., 1995, *AJ*, 110, 2365
 Bono, G., Caputo, F., Castellani, V., Marconi, M., Storm, J., DeglInnocenti, S., 2003, *MNRAS*, 344, 1097
 Bramich D. M., Horne K., Bond I. A., Street R. A., Cameron A. C., Hood B., Cooke J., James D., Lister, T. A., Mitchell D., Pearson K., Penny A., Quirrenbach A., Safizadeh N., Tsapras Y., 2005, *MNRAS*, 359, 1096
 Bramich, D. M. 2008, *MNRAS*, 386, L77
 Burke, E.W., Rolland, W.W., Boy, W.R., 1970, *JRASC*, 64, 353
 Cacciari, C., Clementini, G., 2003, *LNP*, 635, 105
 Cacciari, C., Corwin, T.M., Carney, B.W., 2005, *AJ*, 129, 267
 Carretta, E., Gratton, R. G., Clementini, G., Fusi Pecci, F., 2000, *ApJ*, 533, 215
 Castelli, F., 1999, *A&A*, 346, 564
 Chaboyer, B., 1999, in *Post-Hipparcos Cosmic Candles*, eds. A. Heck & F. Caputo (Dordrech: Kluwer), p. 111
 Clement C. M., Muzzin, A., Dufton, Q., Ponnampalam, T., Wang, J., Burford, J., Richardson, A., Rosebery, T., Rowe, J., Hogg, Sawyer-Hogg H., 2001, *AJ*, 122, 2587
 Clementini, G., Gratton R. G., Bragaglia, A., et al. 2003, *AJ*, 125, 1309
 Dotter, A., Chaboyer, B., Jevremović, D., Baron, E., Ferguson, J. W., Sarajedini, A., Anderson, J. 2007, *AJ*, 134, 376
 Cox, A. N., Hudson, S. W., Clancy, S. P., 1983, *ApJ*, 266, 94
 Dworetzky, M. M., 1983, *MNRAS*, 203, 917
 Di Fabrizio, L., Clementini, G., Maio, M., Bragaglia, A., Carretta, E., Gratton R. G., Montegriffo, P., Zoccali, M., 2005, *A&A*, 430, 603
 Freedman, W.L., Madore, B.F., Gibson, B.K. et al. 2001, *ApJ*, 553, 47
 Gratton R. G., Bragaglia, A., Clementini, G., Carretta, E., Di Fabrizio, L., Maio, M., Taribello, E., 2004, *A&A*, 221, 937
 Geisler, D., Piatti, A.E., Clariá, J.J., and Minniti, D. 1995, *AJ* 109, 605
 Harris, H.C., 1993, *AJ*, 106, 604
 Harris, W.E., 1996, *AJ*, 112, 1487
 Jeon, Y.-B., Lee M.G., Kim S.-L, Lee H., 2004, *AJ*, 128, 287.
 Jurcsik, J., *Acta Astron.*, 1995, 45, 6653
 Jurcsik, J., 1998, *A&A*, 333, 571
 Jurcsik, J., Kovács G., 1996, *A&A*, 312, 111
 Kinman, T.D., 2002, *Inf. Bull. Var. Stars*, No. 535
 Kovács, G., 1998, *Mem. Soc. Astron. Ital.*, 69, 49.
 Kovács, G., 2002, in *ASP Conf. Ser. 265, ω Centauri: A Unique Window into Astrophysics*. Eds. van Leeuwen, F., Hughes, J., Pioto, G., (San Francisco; ASP), p. 163
 Kovács, G., Kanbur, S.M., 1998, *MNRAS*, 295, 834
 Kovács, G., Walker, A.R., 2001, *A&A*, 371, 579
 Lázaro C., Arellano Ferro A., Arévalo M. J., Bramich D. M., Giridhar S., Poretti E., 2006, *MNRAS*, 372, 69
 Lenz, P., Breger, M. 2005, *Communications in Asteroseismology*, 146, 43
 McNamara, D.H., 1995, *AJ*, 109, 1751.
 Marconi, M., Nordgren, T., Bono, G., Schnider, G., Caputo, F., 2005, *ApJ*, 623, 133
 Marín-Franch, A., Aparicio, A., Piotto, G., Rosenberg, A., Chaboyer, B., Sarajedini, A., Siegel, M., Anderson, J., Bedin, L. R., Dotter, A., Hempel, M., King, I., Majewski, S., Milone, A. P., Paust, N., Reid, I. N., 2009, *ApJ*, 694, 1498
 Mannino, G., 1963, *Pub. Obs. Bologna*, 8, 12
 Montegriffo, P., Ferraro, F. R., Origlia, L., Fusi Pecci, F., 1998, *MNRAS*, 297, 872
 Morgan, S.M., Wahl, J.N., Wieckhorst, R.M., 2007, *MNRAS*, 374, 1421
 Nemeč, J.M., 1989, in *The Use of Pulsating Stars in Fundamental Problems of Astronomy*, IAU Coll. 111, ed. E.G. Schmidt, p. 215
 Nemeč, J.M., 2004, *AJ*, 127 2185.
 Nemeč, J.M., Cohen, J.G., 1989, *ApJ*, 336, 780
 Nemeč, J.M., Mateo, M., Schombert, J.M., 1995, *AJ*, 109, 618
 Nemeč, J.M., Linnell Nemeč, A.F., Lutz, T.E., 1994, *AJ*, 108, 222.
 Nemeč, J.M., Mateo, M., Burke, M., Olszewski, E. W., 1995, *AJ*, 110, 1186
 Rodríguez, E., López-González, M. J., 2000, *A&A*, 359, 597
 Rosenberg, A., Saviane, I., Piotto, G., Aparicio, A., 1999, *ApJ*, 118, 2306
 Rosenberg, A., Aparicio, A., Saviane, I., Piotto, G. 2000, *A&AS*, 145, 451
 Rutledge, G.A., Hesser, J.E., Stetson, P.B., 1997, *PASP*, 109, 907
 Salaris M., Chieffi A., Straniero O., 1993, *ApJ*, 414, 580
 Salaris M., Weiss, A., 2002, *A&A*, 388, 492
 Sarajedini, A., Milone, A.A.E., 1995, *AJ*, 109, 269
 Sekiguch, M., Fukugita, M., 2000, *AJ*, 120, 1072
 Simon N. R., Clement C. M., 1993, *ApJ*, 410, 526
 Stetson, P. 2000, *PASP*, 112, 773
 Straniero, O., Chieffi, A., Limongi, M. 1997, *ApJ*, 490, 425

Suntzeff, N.B., Kraft, R.P., Kinman, T.D. 1988, AJ 95, 91
van Albada, T.S., Baker, N., 1971, ApJ, 169, 311
VandenBerg, D.A., Bergbusch, P.A., Dowler, P.D., 2006,
ApJS, 162, 375
VandenBerg, D.A., Bolte, M., Stetson, P.B., 1990, AJ, 100,
445
VandenBerg, D.A., Clem, J.L., 2003, AJ, 126, 778
van den Marel, R.P., Alves, D.R., Hardy, E., Suntzeff, N.B.,
2002, AJ, 124, 2639
Zinn R., 1985, ApJ, 293, 424
Zinn R., West, M.J., 1984, ApJS, 55, 45